Impact of Climate Change on Flood Frequency and Intensity in Washington, DC and its Vegetation: A Case Study of the Potomac River and Anacostia River Watershed

Ying Chen

Bachelor of Science, University of Virginia, 2020

A thesis presented to the Graduate Faculty of the University of Virginia in Candidacy for the Degree of Master of Arts in

Environmental Science

Department of Graduate School of Arts and Sciences

University of Virginia

July 2023

Contents

List of Figures

List of Tables

Acknowledgments

My sincere gratitude and appreciation go to my supervisor, Professor Stephen Macko. Without his invaluable support and guidance, this work would not have been possible. Professor Macko's friendly mentoring and expert advice have shaped and enhanced every aspect of this research endeavor. I would like to extend my sincere gratitude to Professor Pei-Jen Shaner and John Porter. Their extensive discussions and valuable suggestions have greatly contributed to refining and advancing this thesis. I truly acknowledge the invaluable intellectual contributions they have made.

Moreover, I would like to express my deep appreciation for the significant role played by my parents, Hsiu Yueh Yang and Kuang Chu Peng. Their profound love for nature has remarkably influenced my understanding and admiration of environmental science. It is important to highlight that her indirect contribution to this project cannot be measured due to its immense impact.

I appreciate the chance to undertake this research while serving in the Environmental Science Department at the University of Virginia. The support and resources extended by the department were vital in successfully completing this thesis.

Abstract

Heavy precipitation often leads to flooding, causing various adverse consequences, including dam breaks, farmland inundation, property damage, and loss of life, making it a prevalent natural disaster worldwide. With the benefits of timely monitoring and comprehensive coverage, remote sensing has become an essential tool for assessing flood impact. As natural disasters rise worldwide, concerns have grown about the potential link between sea-level rise and flood frequency and whether particular regions are more susceptible to these risks. This research delves into the relationship between sea-level rise and flood frequency, aiming to pinpoint the most vulnerable areas. Additionally, our study explores how floods affect vegetation in the Washington, D.C. region. By leveraging published reports, Excel, remote sensing, and ArcGIS tools. The research thoroughly analyzes flood-prone areas to ascertain the significance of this relationship. The findings of this study may assist in evaluating flood events and provide insight for future research.

1. Introduction

The motivation for the study arises from a significant event in August 2021. During this time, Old Town Alexandria, a historic district situated along the Potomac River, endured severe flooding due to heavy rainfall. As water levels rose, streets, sidewalks, and buildings were engulfed, causing extensive damage to infrastructure, businesses, and residences. This incident emphasized the urgent need to address flood risks and vulnerabilities in the area while emphasizing the importance of implementing effective floodplain management strategies. Therefore, this study aims to explore the link between climate change and flood patterns in the specified watershed area while assessing their impact on local vegetation.

1.1 The reasons of a flood event

Floods, natural disasters when water overflows and covers typically dry lands, can devastate rivers, lakes, offshore areas, and communities, resulting in loss of life and property damage worth billions of dollars (Wu et al., 2022). Heavy rains can trigger floods, dam collapses, excessive sedimentation, and massive meltwater flow from collapsing glacial lakes (Guan et al., 2015). These events can cause significant damage to homes, bridges, roads, and infrastructure, as well as destroy crops and claim lives. Although periodic flooding benefits floodplain soils by maintaining nutrient balance, frequent or more extensive floods can harm water quality. They displace aquatic organisms, increase soil erosion, and degrade overall water quality (Haasnoot et al., 2020).

Flood formation involves various factors, as depicted in Figure 1: The primary factor is increased water sources like rainfall, snow melting, storm surge, and tsunamis. The second factor involves the disruption of environmental elements, such as unstable river basins, damaged dams,

insufficient vegetation, limited watershed capacity, and inadequate surface management. When the primary factor exceeds the capacity of the environment to handle it, a flood event can occur. However, other contributing factors can also lead to an environmental breakdown that results in flooding.

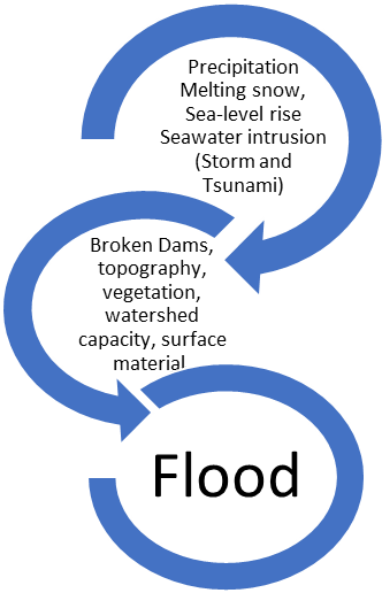

Figure 1: The main causes of flood formation, on the top level of the circle shows the water sources, and the second shows the environmental reasons.

The major factor : water source

Heavy rains: One of the most straightforward explanations for floods is heavy rains. Typically, systems and infrastructure are in place to manage rainwater by directing it to reservoirs and basins, which typically work well. However, during intense rainfall, these systems may become overwhelmed, causing water to accumulate and resulting in floods due to their limited capacity (Lopez et al., 2017).

Storm surges, tsunamis, melting ice, and snow: Floods can be triggered by various factors beyond rainfall. Storm surges from storms and hurricanes, and tsunamis resulting from underwater earthquakes can also lead to flooding (Mikhailova, 2021). Heavy snowfall and melting ice also contribute to floods, requiring adequate drainage to prevent overflow (Sundaram et al., 2022).

The second factor: environment

Overflowing rivers: Flooding does not always require heavy rainfall. For example, areas along a river can experience harsh overflow due to heavy rainfall in upstream areas, even if the immediate area does not experience heavy rainfall (Merz et al., 2021).

Broken Dams: The rise in water levels caused by heavy rainfall can lead to the failure of aging dams and release torrents of water on unprepared households. The catastrophic floods caused by Hurricane Katrina in 2005, which resulted from the failure of levees, serve as a stark reminder of this phenomenon (Mensah & Ahadzie, 2020).

Urban Drainage Basins: In urban areas, concrete-based drainage basins are commonly used due to impermeable surfaces. When these basins become overwhelmed with water, it hinders water from seeping into the ground, flooding nearby low-lying areas (Liu et al., 2019).

Channels with Steep Sides: When rivers or lakes have steep sides, fast runoff can lead to flooding, especially in narrow channels (Singh & Patil, 2021).

Lack of vegetation: Vegetation is vital in slowing runoff and minimizing flooding risks. Without sufficient vegetation, natural barriers that can slow or halt water flow are lacking (Dahri & Abida, 2020).

Urban planning: Impervious surfaces like roads, parking lots, rooftops, and concrete can impede infiltration and increase surface runoff, affecting water flow toward nearby rivers (Lee et al., 2012).

Recognizing the connection between flooding events and coastal change holds great importance, as underscored by the Intergovernmental Panel on Climate Change (IPCC, 2014). In one of their special reports on extremes, the IPCC (2014) affirms that" **climate change has become increasingly evident in its impact on various water-related factors contributing to floods, including rainfall and snowmelt.**" (cited in Lionello et al., 2021, p. 2633). Moreover, comprehending the causes by which climate change contributes to flooding, including heavier precipitation, more frequent hurricanes, rising sea levels, and other factors, is crucial (Haasnoot et al., 2020).

1.2 Inland flooding and coastal flood

Inland flooding can occur due to various factors, such as rapid rainfall exceeding the watershed or valley drainage capacity, melting snow, mudslides, and uncontrolled water release from dams or river banks. Additionally, structural collapses from natural flow or non-hydrological events like earthquakes, technological failures, or sabotage can trigger flooding (Hunt, 2005). Thus, it is crucial to carefully assess the risk of potential inland flooding to evaluate overall flood risk.

Coastal flooding happens when seawater or surface runoff submerges low-lying land (Ramsay and Bell, 2008). Strong winds and high tides lead to flooding of coastal plains and damage to fortifications. The extent of damage depends on the types of structures in place. Hard structures like dikes, seawalls, breakwaters, groynes, or jetties may survive or be destroyed, while more

flexible structures like dunes or marshes can be relocated and restored (Pin-Chun Huang, 2022). However, even natural defenses cannot withstand very severe storms that cause rapid changes to coastlines.

Simultaneous or sequential occurrences of both inland and coastal flooding can result in severe consequences. In the event of a coastal storm surge, if high rainfall and rising inland river levels follow, coastal flooding can be doubly severe (Ray et al., 2011).

1.3 Temperature, sea-level and flooding record

Rising air temperature

According to the National Oceanic and Atmospheric Administration (NOAA), the global temperature has been rising by an average of 0.14 degrees Fahrenheit per decade since 1880. In the contiguous 48 states of the United States (as depicted in Figure 2), temperatures have increased at an average rate of 1.35 degrees Fahrenheit per decade since 1895. Notably, the year with the highest recorded temperatures was 2021, reaching an average of 72.59 degrees Fahrenheit.

Temperature acts as a vital gauge for assessing how global climate change impacts ecosystems and human life. The Intergovernmental Panel on Climate Change (IPCC, 2014) has affirmed that this temperature increase primarily stems from human activities, including the burning of fossil fuels, deforestation, and industrial processes. These activities release greenhouse gases and trap heat in the atmosphere, and rise in temperature has resulted in a wide array of consequences, such as the melting of glaciers, the escalation of sea levels, the occurrence of more frequent and

severe heat waves, alterations in precipitation patterns, and more extreme weather events (IPCC, 2014).

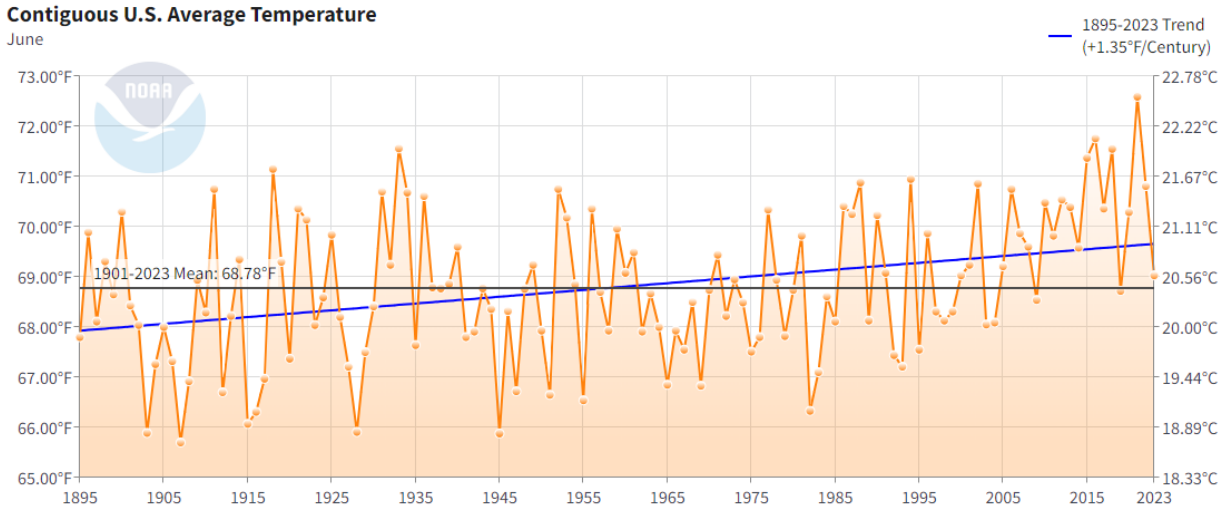

Figure 2: Average temperature record in the contiguous 48 states from 1895 to 2023. (Source: https://www.ncei.noaa.gov/access/monitoring/climate-at-a-glance/)

Rising sea level

According to NOAA, sea level rise is a pressing concern. Figure 3 displays seasonal sea level estimates from Church and White (2011) covering 1880 to 2020, along with data from the University of Hawaii Sea Level Center from 1970 to 2020, and they consistently match. Since the 1880s, sea levels have risen by approximately 20.3 to 22.9 cm, with an increasing rate since 1950 and a faster pace since 2000. By 2020, sea levels reached a new record high of 9.1 cm above 1993 levels, indicating a continuous acceleration in sea level rise. The global sea level rise rate has increased from about 0.175 cm per year in the 20th century to approximately 0.33 cm per year from 1993 to 2020 (Tebaldi et al., 2021). This emphasizes reducing greenhouse gas

emissions and addressing climate impacts to prevent further intensifying sea-level rise consequences.

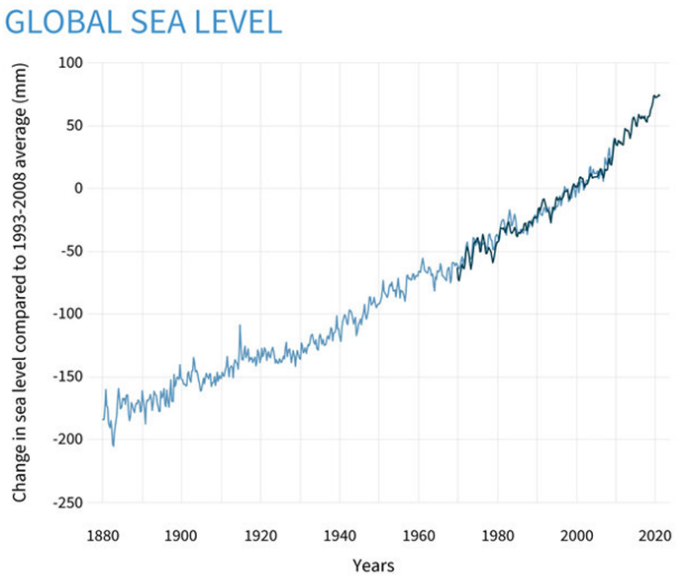

Figure 3: The trend line shows the comparison between seasonal sea level estimates (Church and White (2011)) between 1880 to 2020 (light blue line) and the University of Hawaii Sea Level Center between 1970 to 2020 (dark blue line).

Source:

https://www.climate.gov/news-features/understanding-climate/climate-change-global-sea-level#:~:text=Global%20average%20sea%20level%20has,3.8%20inches)%20above%201993%20levels.

Increased rainfall events

General statements about global rainfall patterns are challenging as they vary significantly across different regions. Some areas, such as tropical regions, are experiencing more frequent and intense rainfall, whereas others are encountering more prolonged and frequent droughts, such as

Sub-Saharan Africa. Rainfall patterns are primarily determined by the local climate and their impact on atmospheric circulation patterns, which human activities and land use can influence (Ohba et al., 2019). In the last hundred years, the frequency and intensity of heavy rainfall events have seen a noticeable rise. According to the NOAA, the percentage of land area in the 48 states that have experienced single-day precipitation events exceeding historical levels has increased from 1910 to 2020. Figure 4 shows that most extreme single-day precipitation events have occurred since 1996. However, the changes in rainfall patterns are complex and regionally variable, and thorough analysis and monitoring are necessary to comprehend their causes and effects.

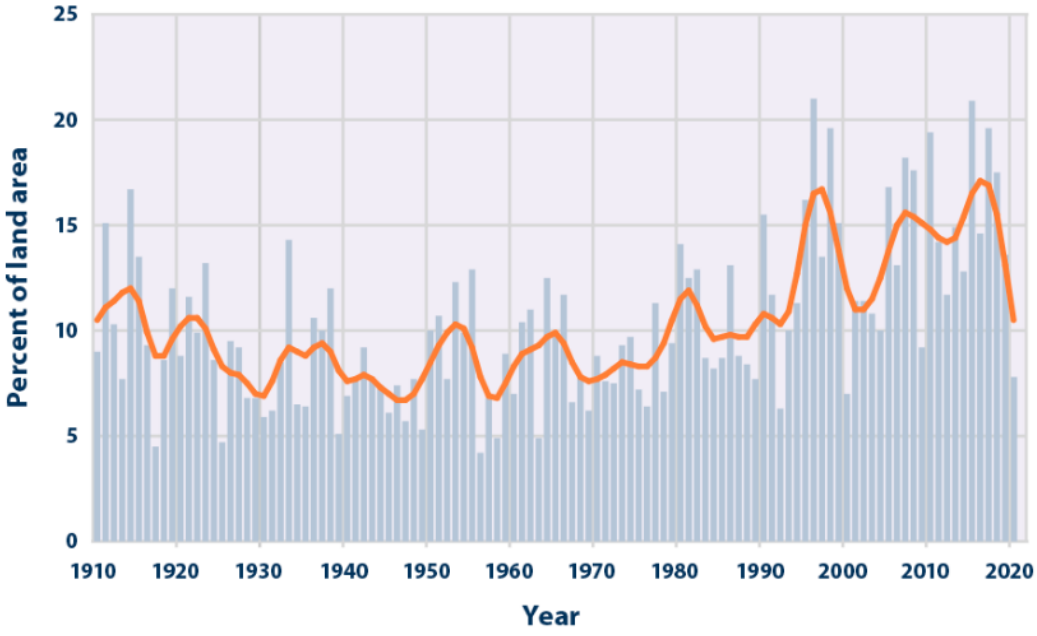

Figure 4 : Extreme one-day precipitation Events in the Contiguous 48 States, 1910–2020, each bar indicated individual years and the line is a nine-year weighted average. (Source: https://www.ncei.noaa.gov/access/monitoring/climate-at-a-glance/)

Increased flooding

The National Oceanic and Atmospheric Administration (NOAA) has recently reported an increase in weather and climate disasters, particularly flooding. Analysis of data from NOAA's Figure 5 reveals significant changes in the size (Figure 5a) and frequency (Figure 5b) of flooding events in streams and rivers across the United States throughout five decades, from 1965 to 2015 (Slater et al., 2016). Notably, regions in the Northeast and Northwest have witnessed a rise in flood sizes, while other areas have experienced a decrease. Moreover, the Northwest, Midwest, and Northeast also observed a considerable surge in flood frequency. Conversely, certain regions displayed only a slight reduction. Overall, the United States is experiencing a growing concern about increased flooding, which is attributed to climate change and other factors (National Climate Assessment, 2018).

(a)

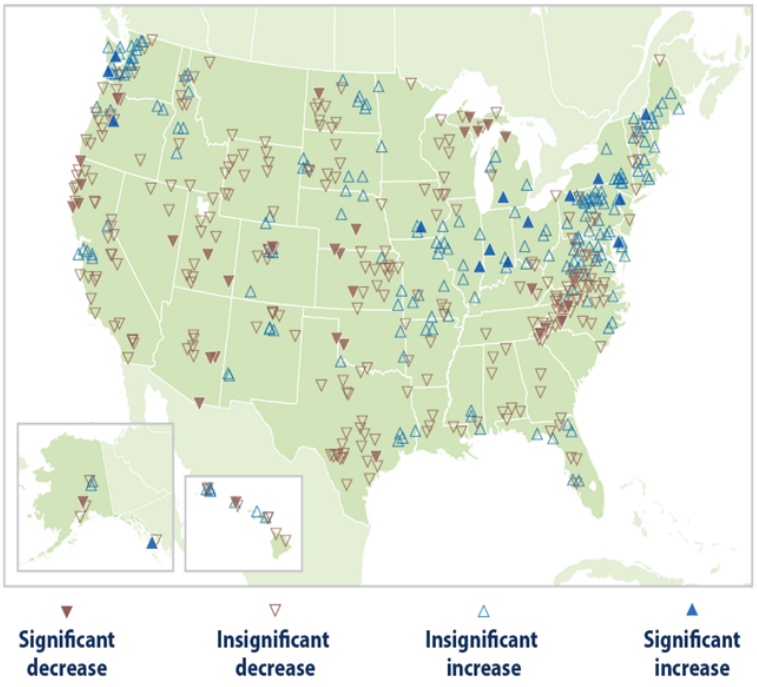

(b)

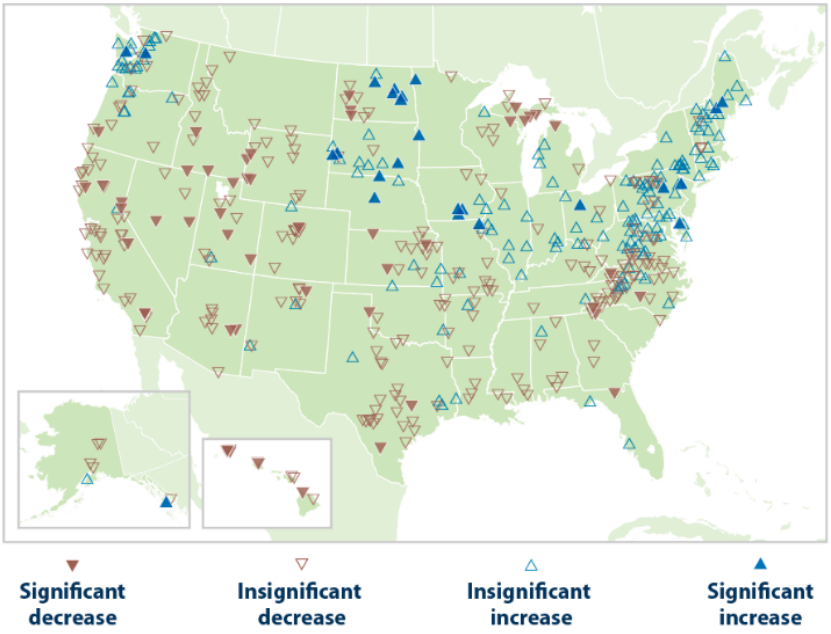

Figure 5: (a) River flood magnitude change in the United States from 1965 to 2015. (b) River flood frequency changed in the United States from 1965 to 2015 (NOAA). (Source: https://www.epa.gov/climate-indicators/climate-change-indicators-river-flooding)

1.4 Temperature increases drive other environmental changes

The global warming rate has significantly increased, and this warming trend leads to more frequent and intense weather events (IPCC, 2018). One of the impacts of climate change is its effect on heat waves. The rise in temperature increases the chances of experiencing scorching days and nights. Climate warming affects land evaporation, which can worsen drought conditions and elevate the risk of wildfires (Xiaoxinet al., 2017). Additionally, a warmer climate may also give rise to heavier precipitation events like blizzards and storms due to increased moisture capacity in the air (Sweet et al., 2014). The moist and warmer atmosphere and warmer

oceans indicate that solid hurricanes will be intense (Walsh et al., 1998). They can produce more rainfall, impact new areas, and be more significant and long-lived. There is evidence from the North Atlantic that tends to support such claims (Vitousek et al., 2017).

Extreme weather events could become more frequent or intense due to climate change caused by activity, according to the IPCC in 2014. It has been observed that the years with the recorded temperatures have also experienced catastrophic consequences, as reported by NOAA in 2023. Elevating temperatures significantly influence the onset of extreme weather events, with a particular impact on heavy rainfall, thereby amplifying the likelihood of flooding incidents (Karl et al., 2008). Each 1-degree Celsius rise in temperature results in a 7% expansion in the air's moisture-holding capacity, leading to heightened evaporation from both land and oceans (Held et al., 2006). This ultimately affects precipitation frequency and volume resulting in a likelihood of rainfall events and an overall increase in flood frequency and intensity (Intergovernmental Panel on Climate Change, 2014).

This combination of climate changes is widely believed to be responsible for rising sea levels contributing to flooding and erosion risks for lying and coastal areas. As the generation continues into this era of climate change, it is evident that flooding incidents are already rising due to the increasing sea levels (Vitousek et al., 2017). The expected continuation of the rise in mean sea level will result in a sustained high coastal water level, causing coastal erosion and flooding in many locations. The public often focuses on the magnitude and rate of mean sea level increase. However, freak waves and storm surges and their timing concerning the astronomical tide fundamentally influence coastal flooding and erosion. Studies have shown that these cumulative impacts, such as storm surges and significant mean sea level rise, pose severe concerns as they can significantly contribute to flooding hazards and catastrophic events (Little et al., 2015).

Therefore, it is critical to examine how sea level rise affects high-frequency flood levels and high-vulnerability areas and the impacts of flood events.

The research unequivocally proves that rising air temperature is the driving force behind heavier precipitation and rising sea levels, significantly increasing the frequency of floods. A meticulous analysis is conducted in the District of Columbia to delve into the precise impact of temperature on flood occurrence.

2. Literature Review

2.1 The relation between sea-level rise and flood frequency

The rise in sea level has a direct impact on flood probability and intensity. When estimating future flood risk, the focus is often on the average, best, or large quantile, but uncertainty in sea level forecasts is not always taken into account. However, factoring in the uncertainty of sea-level rise increases the probability of flooding (Ruckert et al., 2017). In the short term, there is only a small increase or no change in the expected conditions of Bothnian Bay and the Gulf of Finland due to stronger land uplift. However, the long-term scenario of rising mean sea levels is predicted to clearly increase flooding risks by 2100. Low-lying coastal areas in Germany are already facing recurrent flooding events caused by storms. The combination of accelerated sea-level changes and hard coastline defenses would increase the squeeze on the seaward side, damaging the coastal ecosystem. Unfortunately, there is currently no solution for this phenomenon (Sterr, 2008).

Research shows a direct link between sea-level rise and the frequency of massive floods in coastal areas. For instance, Areas with high rainfall are directly impacted by sea-level rise

(Vitousek et al., 2017). As a result, low-lying equatorial and tropical islands will become uninhabitable and submerged by 2050 due to extreme sea and flood frequency. Similarly, sea-level rise increases flooding frequency in coastal regions, directly affecting coastal geomorphology (Al'ala & Syamsidik, 2019). Global climate change altered weather patterns in coastal regions of California, increasing the likelihood of flooding owing to increased rainfall (Dettinger, 2011). Additionally, global sea levels have risen significantly owing to climate change, exacerbating the frequency of flooding on the California coast.

Several research articles have noted different processes by which sea-level rise will influence the increasing rate of flood frequency. Rising sea levels, intensified storms, and tides will increase the risk of flooding in urban areas. The increased exposure to greenhouse gasses leads to greater uncertainties when predicting scenarios for the year 2100 in the San Francisco Bay Area (Yang et al., 2019).

The frequency and intensity of floods have a direct correlation with the availability of water in specific regions and seasons. Regions and seasons with higher moisture availability experience a larger increase in flood events and extreme rainfall. However, in dryer regions, the increase in extreme rainfall may be offset by reduced moisture availability. On the other hand, water-abundant regions with more moisture convergence experience intensified impacts of extreme rainfall. Hence, it is important to take into account both atmospheric conditions and water availability when predicting and preventing floods (Tabari, 2020).

For example, tropical regions are more vulnerable to sea-level rise and coastal flooding due to their high rainfall and seasonal water variability (Vitousek et al., 2017). The rising sea level further exacerbates the water level during high rainfall, increasing the frequency of massive

flood formation. Further, climate change is altering the weather patterns in the coastal regions of California, leading to more incoming warm air and orographic rainfall (Dettinger, 2011). The increased precipitation, combined with sea-level rise, is increasing the frequency of flooding in these regions.

2.2 Areas in danger

The areas along the coastlines are at a greater risk of more floods owing to rising sea levels. Especially, areas with high water variability in tropical regions encounter increased vulnerability, while low-lying islands in equatorial and tropical regions are at even more heightened risk (Vitousek et al., 2017). Shortly, coastal areas will experience more massive flood events, potentially rendering them uninhabitable (Dettinger et al., 2011). Moreover, there is a circumstance that low-lying islands may be submerged by 2050 due to increased sea levels and flood frequency (Al'ala et al., 2019).

These findings demonstrate that the recent increase in massive floods is primarily due to rising sea levels, and prompt mitigation measures are required to protect the world, human society, and biodiversity from the severe consequences of sea-level rise.

2.3 Flood impact on Vegetation

Depending on the severity and the type of flood, it can have both negative and positive effects on vegetation. Here are some potential effects flooding can have on vegetation:

Waterlogging: Waterlogging occurs when floods overwater the soil, reducing soil porosity and causing stress to plants. Waterlogging can cause oxygen deprivation and reduced nutrient uptake availability for plants, leading to reduced root growth and root morphology (Naeem *et al.* 2021).

Soil Erosion: Flooding can cause nutrient loss and soil erosion, which can lead to the reduction of soil fertility and environmental degradation (Yang *et al*., 2021) These are the factors that cause a decrease in vegetation.

Sediment deposition: Flooding events increase sediment deposition and organic carbon storage, rich in organic matter. The soil quality becomes more fertilized, which benefits the plants and increases vegetation (Wu et al., 2022).

The impacts of flooding on vegetation rely on elements like how long and severe the floods are, the types of plants in the area, and their capability to adapt to changing situations. Vegetation can be helpful during floods by absorbing extra water, preventing soil erosion, and enhancing soil quality. However, flooding can also harm vegetation through waterlogging and soil erosion, reducing root growth and less vegetation overall. Studying how flooding affects vegetation helps us better understand its impact on ecosystems and find ways to reduce its negative consequences.

2.4 Study Area

This study focuses on the Washington DC area, which has many impermeable surfaces, Figure 6. That means the ground surface of the area has more difficulty handling large amounts of rainwater falling in a short period. In addition, the location of the District of Columbus is at the confluence of two tidal rivers. Hence, the downtown area and the surrounding suburbs experience three significant types of flooding: interior flood, river flood, and coastal flood.

Internal flood: Also known as flash floods, these floods are mainly caused by heavy rains that tend to take place over a very short period, that is, generally up to six hours or even less, and these floods can take place anywhere (Kirezci et al., 2020). The ground cannot absorb the heavy

rain and floods the drainage system. When the river elevation is average, waterlogging may occur due to factors such as topography, development, local weather, and the capacity of the stormwater system.

River Flooding: This mainly takes place when a stream or a river manages to overflow its natural banks as well as tends to inundate dry land (Dahri and Abida (2020). In the Washington area, it refers to overbank flooding on the Potomac River and Anacostia River, when it cannot contain the water collected in its river basin. Heavy rainfall or snowmelt upstream would cause the water level in the lower Potomac River to rise within a few hours or days, which may also cause the backwater of the Anacostia River to overflow.

Coastal Flooding: This type of flooding occurs when the winds that emerge from the coastal storm manage to push a storm surge from the ocean and to the land (Hague et al., 2020). In the Washington area, it refers to the inundation caused by the connection of the Potomac and Anacostia rivers with the Chesapeake Bay and the Atlantic Ocean. Coastal floods include floods caused by high tides, but also include coastal storms, such as hurricanes, that push storm surges, and waves on the Potomac River and Anacostia River into Washington, DC.

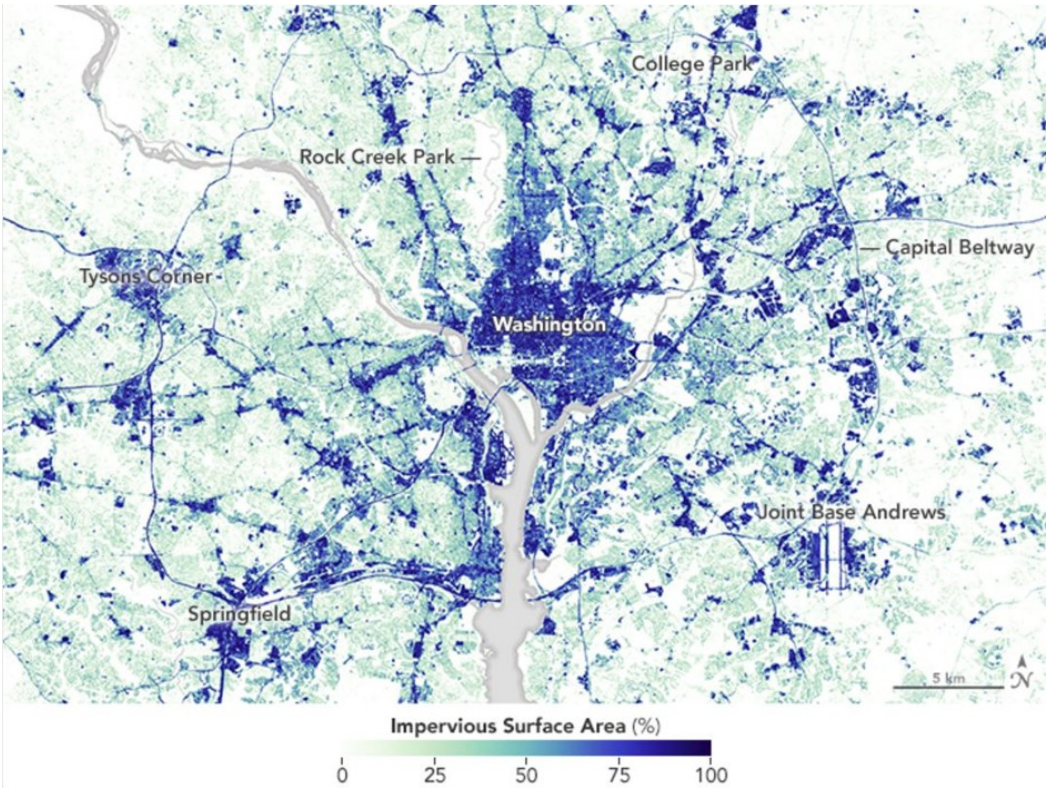

Figure 6 : The distribution of impervious surfaces in the Washington DC area in 2020, as observed by satellite imagery. Map by Metcalfe, J. 2016 (Metcalfe, J,2016). Retrieved from https://www.bloomberg.com/news/articles/2016-03-30/the-growth-of-impervious-surfaces-in-washington-d-c-as-seen-by-satellite

3. Methodology

3.1 Research Design

Qualitative, analytical, and predictive research strategy designs achieve the objectives. Excel, ArcGIS, and Google Earth Engine were used to approach this study due to the research question's exploratory and qualitative nature in focus. This study uses frequency analyses to predict design floods for sites along the Potomac and Anotacia Rivers. The analysis requires the

observed annual peak flow data in the history to calculate statistics and then construct the frequency distributions.

3.2 Research Approach and Strategy

The research methodology used in this study involves a systematic approach. It starts with general assumptions, such as the positive correlation between temperature increase and flood frequency, and then proceeds to collect data from government sources. The study analyzes the data using frequency distribution and presents the results in graphical and tabular formats. The study adopts an inductive research approach, focusing on specific observations and data to draw broader conclusions relevant to the research design.

3.3 Data Preparation

The data on temperature, sea level, precipitation, and stream level in the district of Columbia was collected for the research. The research collected various data types, including temperature, sea level, precipitation, and stream-level data. Reliable sources, such as NOAA for temperature, sea-level, and precipitation data and USGS for stream-level data, provided these. Once the study verified the data, they converted it into a format suitable for analysis in Excel, such as CSV or XLSX. The research utilized a web application, Streamlit, to compare sea-level data with land cover images. They leveraged open-source mapping libraries like leaf map, gee map, pydeck, and kepler.gl to generate an appropriate map for this study. These libraries were applied to generate an appropriate map for this study. Additionally, Google Earth Engine created maps that aided the study in analyzing flood comparison images.

3.4 Data Analysis

Temperature, rainfall and precipitation analysis

The data analysis mainly uses Excel to analyze temperature, rainfall, and precipitation data, creating graphs and examining trends and patterns over time. The study explored seasonal variations and long-term changes to understand climate behavior better. Potential correlations between variables, such as the impact of temperature changes on precipitation and sea level, were investigated.

Image land cover analysis

The study utilizes Streamlit to explore potential connections between historical land cover and sea level. Initially, historical land cover images undergo preparation using image processing techniques for comparison. For accurate flood event monitoring, Google Earth Engine involves diverse satellite images like MODIS, Sentinel-1, and 2. These images were corrected for surface reflectance and collected before and after each flood event. However, remote sensing faces limitations, especially in monitoring flood events. Clouds can obstruct the view of satellite sensors, making it challenging to obtain clear and accurate flood images. Additionally, some satellite rotation periods may not align with flood occurrences, hindering real-time monitoring. Radar is also affected by clouds but to a lesser extent. It operates at longer wavelengths, penetrating clouds to monitor flood-prone areas effectively. However, heavy rainfall during floods can still impact radar measurements, affecting detection accuracy. Nonetheless, radar remains valuable for flood monitoring, complementing optical remote sensing for disaster management and response. Thus, the monitored flood events occurred on specific dates: July 8, 2019; March 15, 2010; and October 26, 2021. It was crucial to select satellites that launched before the event to monitor each flood event and avoid cloud-covering conditions effectively. For

example, Sentinel-2 was used to detect the flood event on July 8, 2019, while MODIS was used to monitor the flood event on March 15, 2010.

Moreover, the recent flood event on October 26, 2021, was detected using Sentinel-1 SAR, which has global coverage every 12 days. Next, the study uses these tools to create interactive maps displaying historical land cover images, allowing users to quickly explore the data and draw insights. By combining these powerful tools, one can better understand how land cover changes may impact sea-level rise and vegetation patterns over time.

Vegetation Observation

The analysis of vegetation changes during flooding events entailed calculating the Normalized Difference Vegetation Index (NDVI) for each image before and after the event using the Google Engine. However, the study had to use different satellites due to variations in their orbits. In addition, a maximum likelihood supervised classification method was applied to determine land cover based on five distinct classes: open water permanent, open water flood, flooded vegetation, urban, and vegetation. The analysis applied False-color images to inform the training period based on 30 regions of interest (ROIs) for each land class, and that allowed for a comprehensive and accurate analysis of vegetation changes before and after flooding events.

Flood Frequency

The flood frequency distributions were calculated using Long-Pearson Type III Distribution equations for statistical analysis. This distribution is widely used by Federal Agencies across the United States to predict design floods. The U.S. Water Advisory Committee on Water Data (1982) recommends this method for flood frequency analysis at river sites. The Log-Pearson

Type III distribution uses historical record data to calculate discharge values for potential future floods, as well as the recurrence intervals for both the Potomac River and Anacostia River. These distribution graphs play an essential role in designing river structures and nearby buildings to protect them against flood events.

The flood frequency curve uses historical data to estimate the return period of flood events and frequency. It plots flow on the y-axis and return period on the x-axis, using a logarithmic scale. Various factors, such as topography, basin characteristics, altitude, channel slope, and meteorological conditions, shape the relationship between the Maximum Mean Daily Discharge and Instantaneous Peak Flow, contributing to each flood event (Fuller et al., 1914).

Typically, flood frequency analysis involves using instantaneous peak flow data, but the graphs can also generate using maximum values of average daily flow data. The statistical analysis uses the Log-Pearson Type III distribution, providing accurate and reliable results for predicting flood frequency and designing structures to withstand future flooding events. This distribution has three parameters: location, scale, and shape, which make it flexible and adaptable to different data sets. Statisticians Carl J. Long and Ralph A. Pearson developed it in the early 20th century, and since then, it has become a widely used tool in hydrology.

The distribution is calculated using the general equation:

$$log\ x = \overline{log\ x} + K\sigma_{log\ x}$$

The equation above uses x to represent the flood discharge value for a given probability, K is a frequency factor which is a skewness coefficient which is found in Table 1 , σ is the standard deviation. To calculate the mean by using the equation: $\overline{log\ x} = \frac{\Sigma(log\ x_i)}{n}$. To calculate the

variance and the standard deviation by using these: $\frac{\sum_{i}^{n}(log\ Q - avg(log\ Q))^2}{n-1}$ & $\sigma\ log\ Q = \sqrt{variance}$; where n is the number of entries.

To calculate the skewness coefficient by using the following equation: $Cs = \frac{n\Sigma(log\ x - \overline{log\ x})^3}{(n-1)(n-2)(\sigma_{log\ x})^3}$.

The value means the estimate incorporates data values, but only from the observing station. When the observations increase, the skewness estimate error would decrease. Another equation which Interagency Advisory Committee on Water Data suggest to estimate the coefficient of skewness for the instantaneous peak flow data by the following equation:

$C_w = WC_s + (1 - W)\,C_m$, where W is a weighting factor $W = \frac{V(C_m)}{V(C_s)+V(C_m)}$, C_m is a regional skewness which would be found in Figure 7. The value of the V(C_m) is 0.302 for the United States (IACWD, 1982). $V(C_s)$ is using the equation to figuring it out:

$V(C_s) = 10^{A - Blog_{10}(n/10)}$,

where

if $|C_s| \leq 0.9$ A=-0.33+0.08 $|C_s|$,

If $|C_s| > 0.9$ A=0.52+0.3$|C_s|$,

If $|C_s| \leq 1.5$ B=0.94-0.26$|C_s|$,

If $|C_s| > 1.5$ B=0.55

Upon calculating all the values, the distribution graph can depict the anticipated discharges to expect at the site in the future based on historical records.

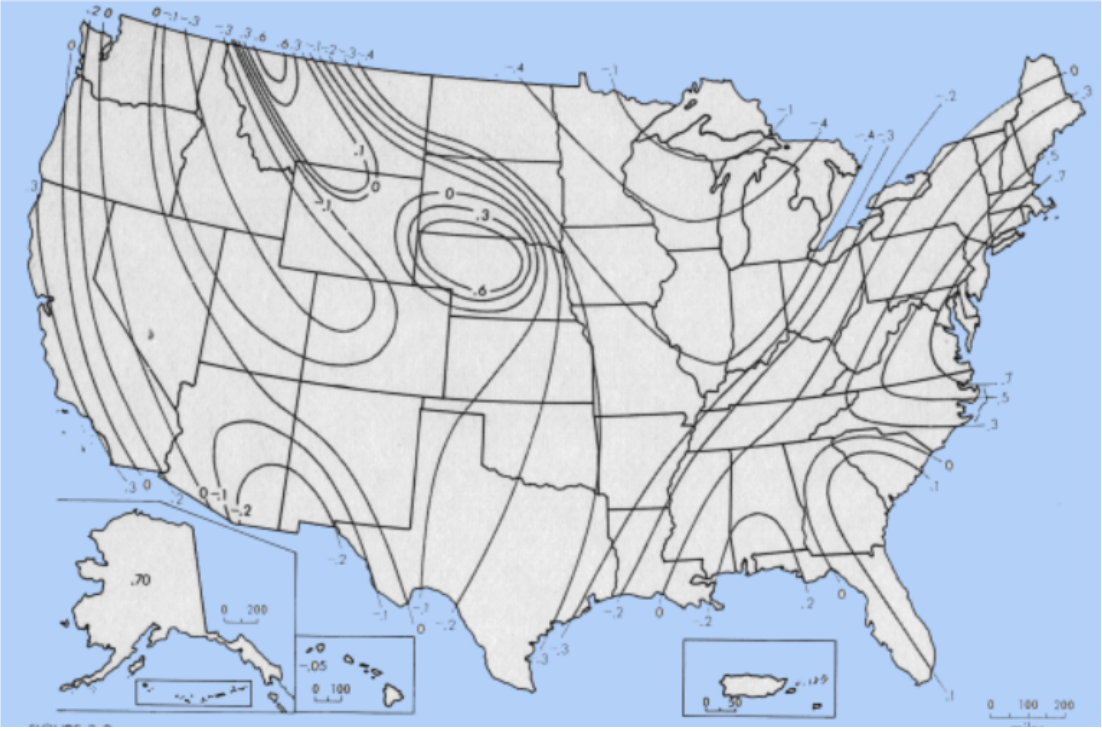

Figure 7: Generalized skew coefficients of logarithms of annual maximum streamflow from interagency Advisory Committee on Water Data, 1982.

Return Period

The return period indicates how often a flood might happen in the future. It is better to talk about return periods than just saying the chance of a flood. Return periods can tell how often a flood of a specific size might happen. For example, a flood with a 100-year return period might happen once every 100 years, but there could still be another big flood in a few years. For example, A flood with a 10-year return period has a 10% chance of happening in any given year.

4. Results

4.1 Rising air temperatures in Washington, DC

The National Oceanic and Atmospheric Administration (NOAA) has been diligently collecting average temperature data in the contiguous District of Columbia from 1871 to 2022. Over the course of 151 years, a notable trend line indicates an increase in temperature by approximately 0.02 degrees Celsius per year (Figure 8). It is essential to consider that local temperatures can be influenced by natural climate variability and urbanization. However, the sustained warming trend observed not only in Washington, DC but also across numerous locations worldwide can primarily be attributed to climate change. This phenomenon is primarily caused by human-induced greenhouse gas emissions, as highlighted by the Intergovernmental Panel on Climate Change (IPCC, 2014), which further expects this trend to persist and intensify in the coming years.

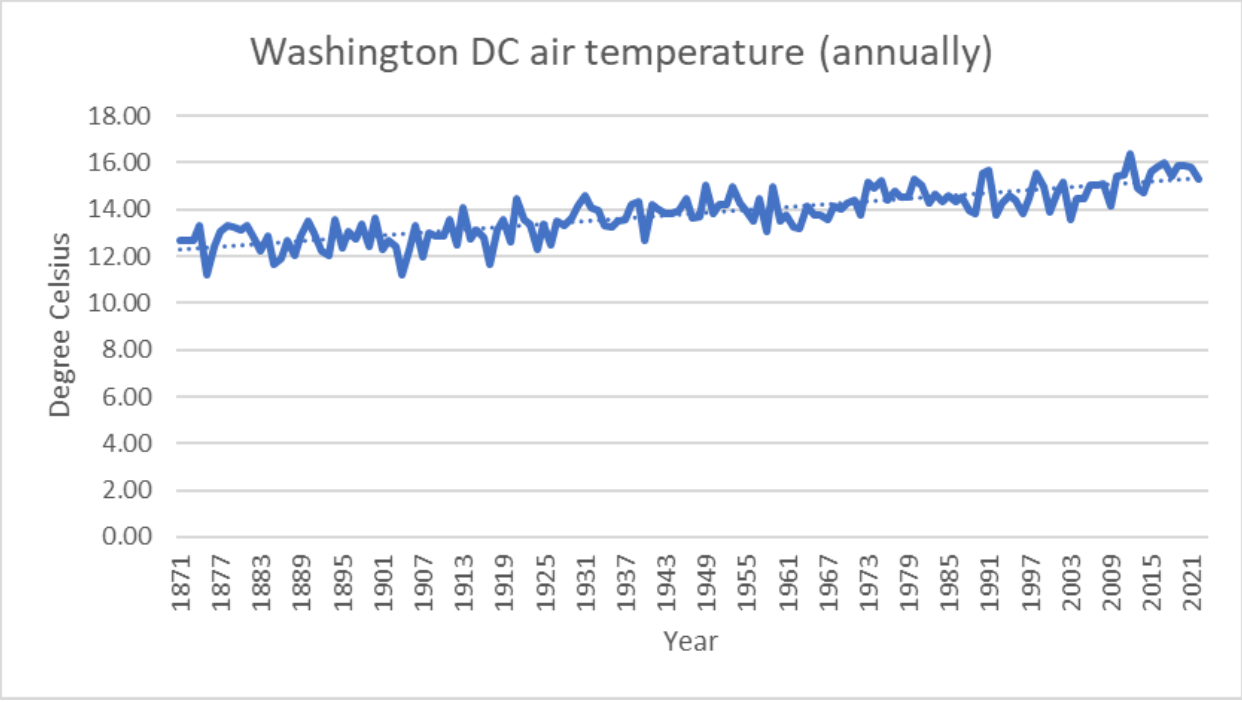

Figure 8: The air temperature in the District of Columbia from 1871 to 2022.

4.2 Rising sea-level in Washington, DC

Sea level rise in Washington, DC, primarily occurs due to the combined effects of melting ice sheets and glaciers and the expansion of seawater amidst global temperature rise. These factors impact the neighboring Chesapeake Bay, contributing to its sea level increase. According to National Oceanic and Atmospheric Administration (NOAA), sea levels have risen by about 3.44 millimeters per year from 1924 to 2021 (Figure 9). Over the last decay, the sea level has risen by around 1.13 feet (or 34 centimeters).

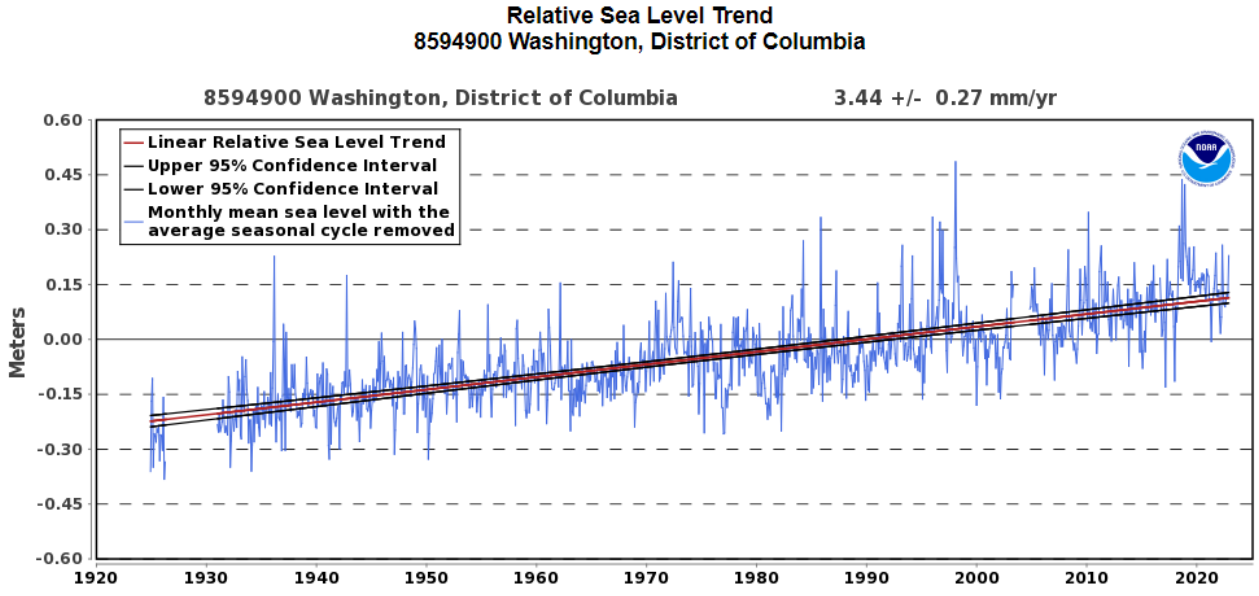

Figure 9: The National Oceanic and Atmospheric Administration (NOAA) provides information on sea level trends in Washington DC. (Source: https://tidesandcurrents.noaa.gov/sltrends/sltrends_station.shtml?stnid=8594900)

Land Cover changes from 1988 to 2020 in Washington, DC

Changes in the District of Columbia from 1988 to 2020 are apparent in the Landsat time Lapse maps made by Streamlit. The natural areas, forests, and agricultural lands are being lost to urban development, as shown in Figure 10. However, sea level rise is not significantly impacting this area because of the district plan. The plan aims to protect the Potomac River shoreline by armoring it from Georgetown to the Lincoln Memorial and constructing a dike to shield low-lying areas between the Lincoln Memorial and the White House from flooding events. While flooding still occurs, the government has built a high levee to minimize economic loss, as Washington DC is the capital of the United States; this could be why the Landsat Time Lapse model does not show the impact of rising sea levels, despite flooding events.

Figure 10: Land changes in Washington DC, from 1988 to 2020. The green color indicated the vegetation, dark blue represents water, white and gray represents road and building. Retrieved from https://geo.streamlit.app/Timelapse?page=Create%20Timelapse

4.3 Rising Rainfall in Washington, DC

NOAA data demonstrates a rise in annual precipitation at both Reagan National Airport and Dulles Airport stations in the Washington D.C. area over the past few decades, and experts predict that this trend will continue in the future (Figure 11(a)). From 1943 to 2023, Reagan National Airport experienced an average annual precipitation of 40.4 inches (Figure 11(b). In contrast, Dulles Airport recorded 41.7 inches from 1965 to 2023, with a notable increase in rainfall during recent years. This increase can be attributed to multiple factors, including higher temperatures leading to increased moisture content in the atmosphere due to greater evaporation and shifts in atmospheric circulation patterns. Furthermore, research suggests that climate change is contributing to more frequent occurrences of intense rainfall events which may result in flooding, infrastructure damage, and other significant impacts. Therefore, several factors contribute to increased rainfall in Washington, D.C. Warmer temperatures result in higher atmospheric moisture content through increased evaporation. Additionally, changes in atmospheric circulation patterns play a role. This research also highlights the impact of climate change on extreme rainfall events, posing risks of flooding and infrastructure damage. It is crucial to acknowledge how these changes affect the weather patterns in the region.

(a)

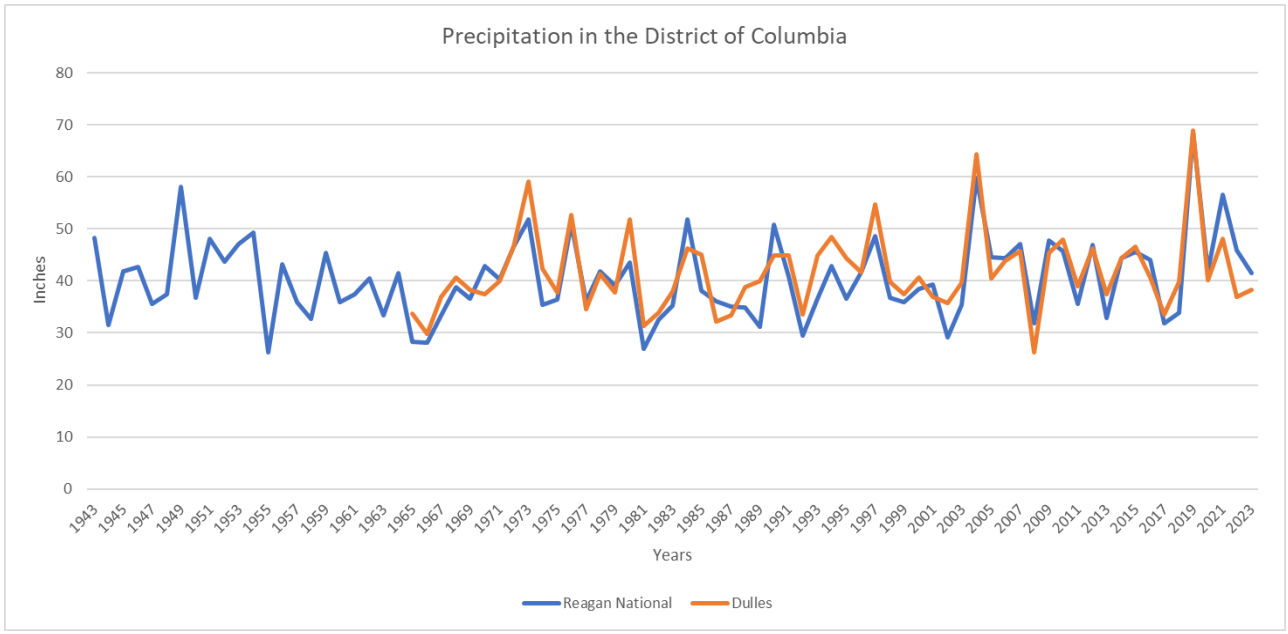
Precipitation in the District of Columbia
Inches
Years
Reagan National
Dulles

(b)

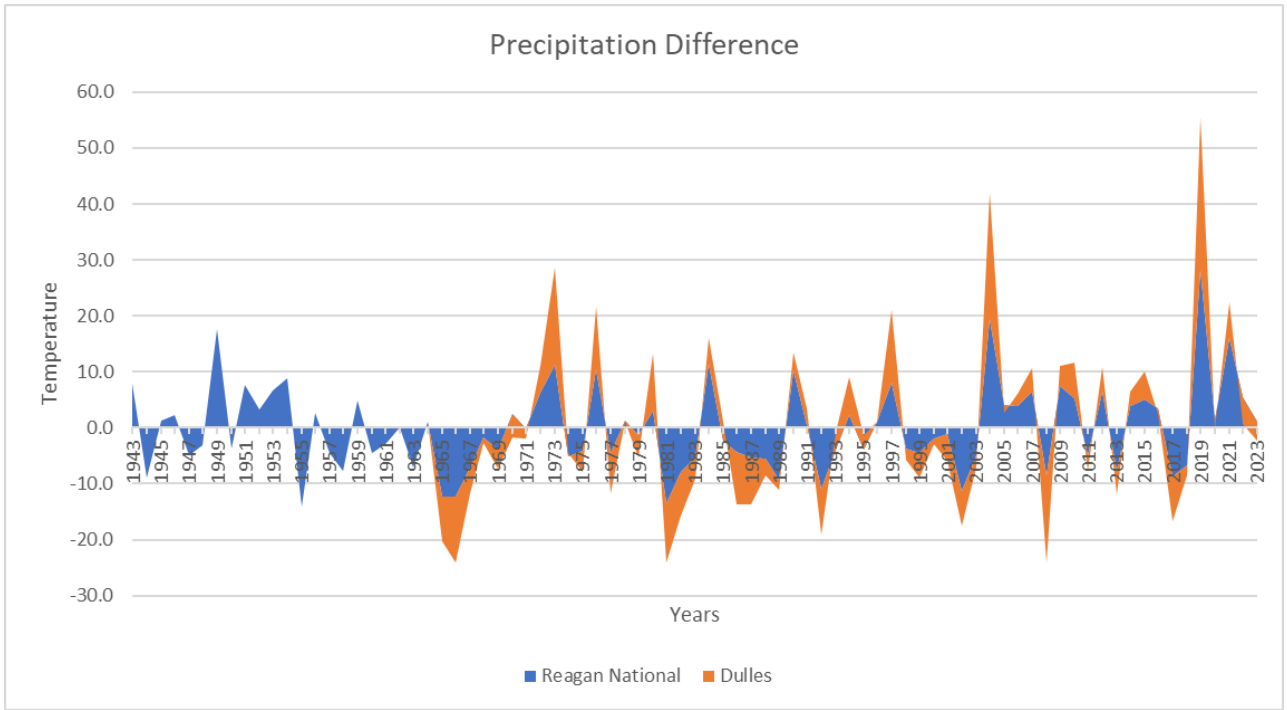
Precipitation Difference
Temperature
Years
Reagan National
Dulles

Figure 11: History precipitation trend at both Reagan National and Dulles airport station from 1943 to 2023. (Data source: https://www.ncei.noaa.gov/access/monitoring/climate-at-a-glance/city/time-series/USW00013743/pcp/12/1/1895-2023)

4.4 Raising Flood Frequency

Instantaneous Peak Flow vs. Maximum Mean Daily Discharge

The Potomac River Little Falls Pump Station, located near the Washington DC metropolitan area, has been the subject of extensive hydrological studies, including measurements of instantaneous peak flow and maximum mean daily discharge. Calculating these measurements, shown in Figures 12 (a) & (b), using historical discharge data from 1931 to 2021 to generate the return period, which expresses the values in cubic feet per second (cfs) and provides critical information for flood control and water resource management. Figure 12 (a) reveals that the instantaneous peak flow for a 2-year return period is approximately 114000 cfs. In contrast, the values for the 10-year, 50-year, 100-year, and 200-year return period floods are much higher, at 228100 cfs, 360000 cfs, 427000 cfs, and 500000 cfs, respectively. Figure 12 (b) shows that the maximum mean daily discharge values for these same return periods are lower, ranging from about 216000 cfs to 494000 cfs. These data are essential for understanding the behavior and developing effective strategies to mitigate the impact of severe floods.

Like the Potomac River, the Anacostia River, situated near Washington, DC, has undergone hydrological investigations to identify its instantaneous peak flow and maximum mean daily

discharge. The unit for the flow is in cubic feet per second (cfs) (Figure 12(b)). According to the data, the instantaneous discharge for a 2-year return period is approximately 3900 cfs. In contrast, the discharge values for 10-year, 50-year, 100-year, and 200-year return period floods are 8000 cfs, 12700 cfs, 14800 cfs, and 17000 cfs, respectively. The average discharge values for these equivalent return periods are comparatively lower, varying from around 3300 cfs to 6500 cfs. These figures hold significant importance in comprehending the behavior of the Anacostia River and in devising strategies to minimize the effects of floods. The Anacostia River exhibits notably lower discharge values than the Potomac River, suggesting it might be less susceptible to flooding. Nevertheless, the data obtained from these hydrological measurements are essential for efficiently managing water resources in the region.

(a)

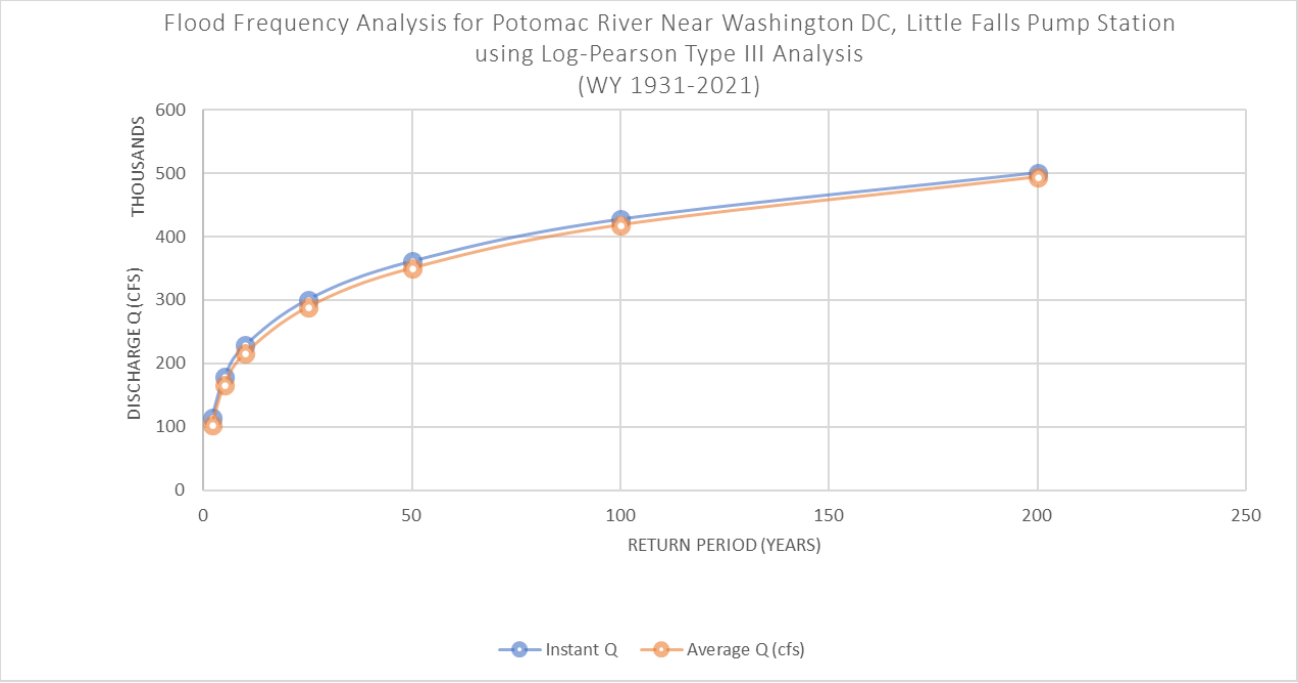

(b)

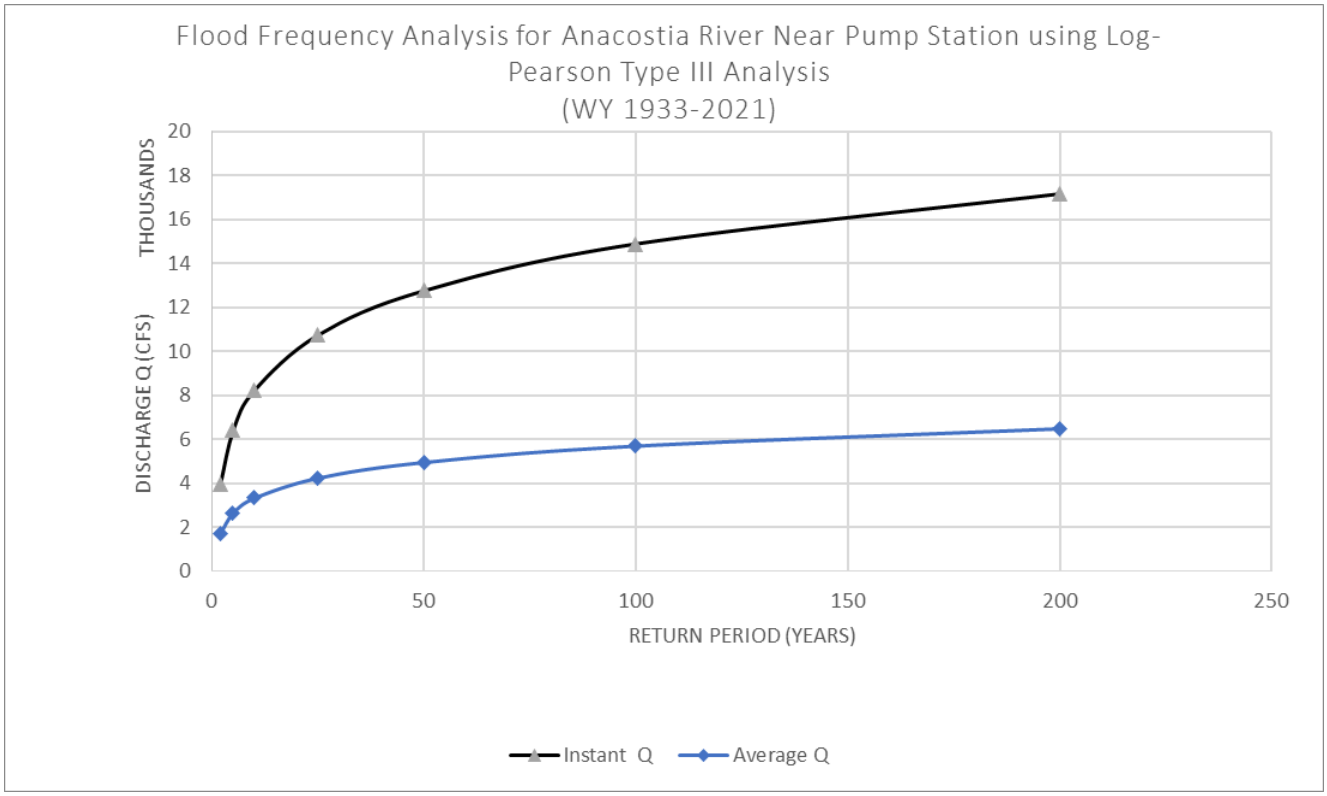

Figure 12 (a) and (b): The flood frequency analysis calculated by Log-Pearson type III analysis on both Potomac River (a) and Anacostia River (b).

The River Gage Height

The Potomac and Anacostia Rivers near Washington, DC, have been investigated to determine their flood event levels. Figure 13 shows the gage height of the stream flow, which helps as a basis for deciding the flood event level mentioned in Table 1. Over time, the gage height of the Potomac River has dropped, while the Anacostia River has stayed unchanged. This flood-level disparity can be attributed to the higher water-holding ability of the Potomac River than the Anacostia River. Therefore, the National Weather Service has established distinct standards for flood levels, representing a gage height above 16 ft as a major flood for the Potomac River.

According to Table 1, the Anacostia River has a slightly elevated standard. An analysis of data transiting the past 91 years shows 51 flood events in the Potomac River and 39 in the Anacostia River, with ten major flood events occurring in the Potomac River but none in the Anacostia River, as indicated in Table 2. This information plays a vital role in comprehending flood risks in the region and devising effective methods to mitigate the influence of floods on emergency planning, flood insurance rates, and infrastructure investments.

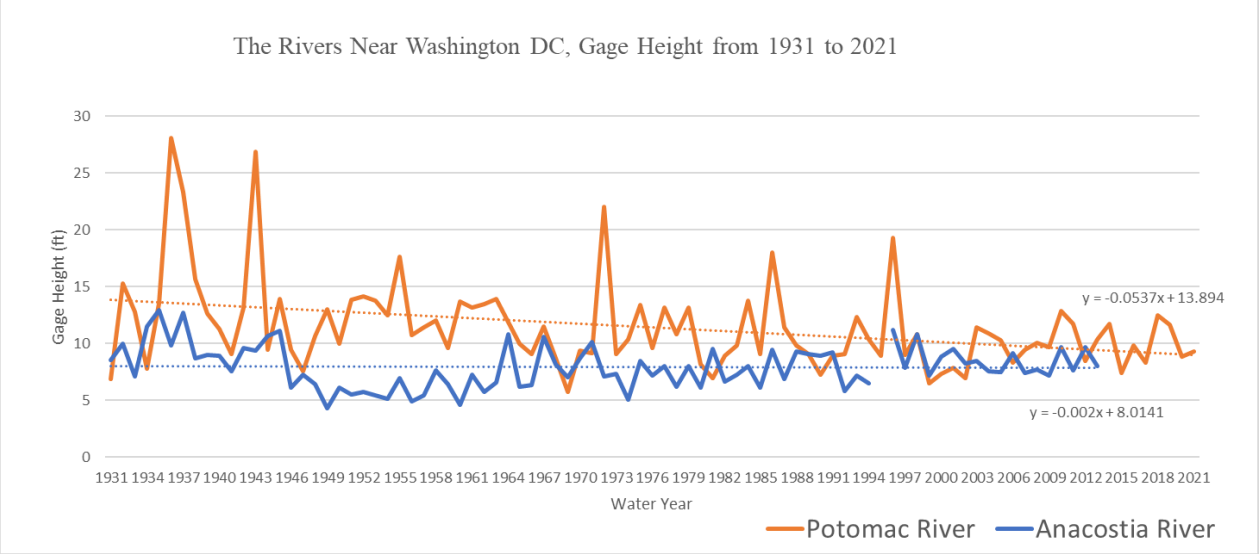

Figure 13: The Gage Height and Stream Peak flow in both Potomac River and Anacostia River. Data retrieved from NOAA.

Standard	Anacostia River	Potomac River
Flood level	Gage Height	Gage Height
Major	16 ft (7891	14 ft (212000 cfs)

	cfs)	
Moderate	13 ft (6651 cfs)	12 ft (163000 cfs)
Flood	8 ft (5411 cfs)	10 ft (114000 cfs)
Action	7 ft (4336 cfs)	5 ft (21000 cfs)

Table 1: The National Weather Service provided the standard table to determine the flood level. Data retrieved from NOAA.

Flood Level	Anacostia River	Potomac River
Major	0	10
Moderate	1	20
Minor	38	21
Action	19	40
Grand Total	58	91

Table 2: The counts of each flood level in both Anacostia River and Potomac River from 1930s to 2021 (yearly stream peak). Data retrieved from NOAA.

Flood Frequency and Its Season

The US Geological Survey (USGS) collects flood frequency data from water stations across the country, but since there is no daily gage height data available for the Northwest Branch Anacostia River at Riverdale MD station, data from the downstream Anacostia River Aquatic

Gardens at Washington, DC daily gauge heights station was used. However, this data is only available from 2004 to 2017, as shown in Figure 14, which indicates that there was only one gage height record reaching action level on February 24th, 2016, with a gage height of 6.3 feet. Since the timeline is not short and able to provide flood frequency information, the focus is shifted to the Potomac River during this time.

Flood events were more frequent between 2008-2011 and 2016-2019, but the trend line indicates a decreasing trend for both moderate and flood levels from 2007 to 2020 (Figure 15 (a)). However, when the gage height reaches above 5 feet in the Potomac River, the action level shows an increasing trend in flood frequency from 2007 to 2021, as shown in Figure 15 (b). Even though the frequency of flood events decreased, the gage height remained at the action level after 2016, indicating an increase in water in the river.

When looking at the water amount specifically, Figure 16 (a) shows a histogram of the number of action water level occurrences for each month from 2007 to 2021 in the Potomac River. The pie chart in Figure 16 (b) shows a 19% chance of the water level remaining at the action level in May but only a 1% chance in July. Factors like precipitation patterns and snowmelt could influence the seasonality of the flood events observed in the Potomac River. For example, higher rainfall in May might lead to more frequent occurrences of gage heights reaching the action level. On the other hand, July might have lower rainfall or less snowmelt, resulting in a lower probability of water levels reaching the action level during that time. Other factors, such as upstream reservoir releases or local hydrological conditions, may also affect the observed seasonality.

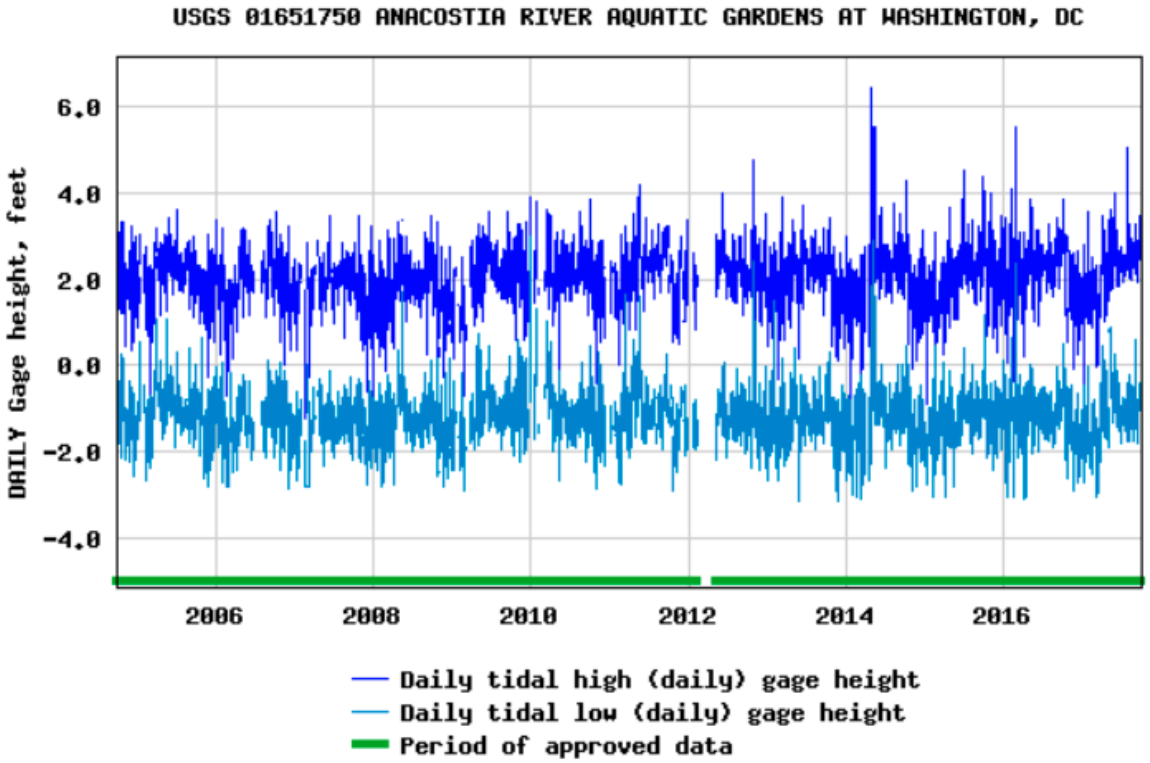

Figure 14: The Daily Gage height in Anacostia River Aquatic Gardens at Washington, DC from 2004 to 2017. Sources: https://waterdata.usgs.gov/nwis/dv?cb_00065=on&format=gif_default&site_no=01651750&referred_module=sw&period=&begin_date=2004-10-01&end_date=2017-09-30

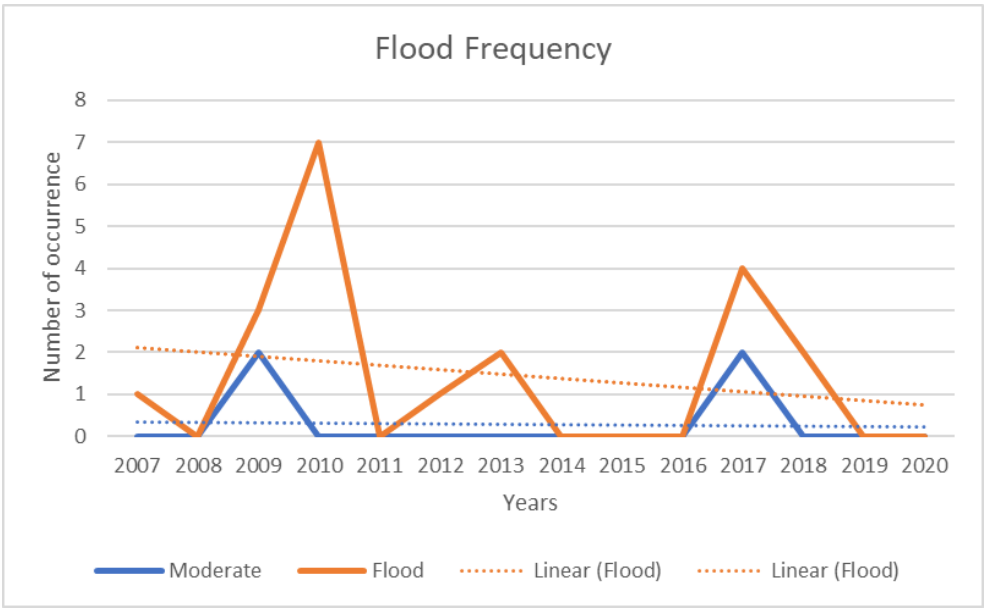
Flood Frequency
Number of occurrence
8
7
6
5
4
3
2
1
0
2007 2008 2009 2010 2011 2012 2013 2014 2015 2016 2017 2018 2019 2020
Years
Moderate
Flood
Linear (Flood)
Linear (Flood)

(a)

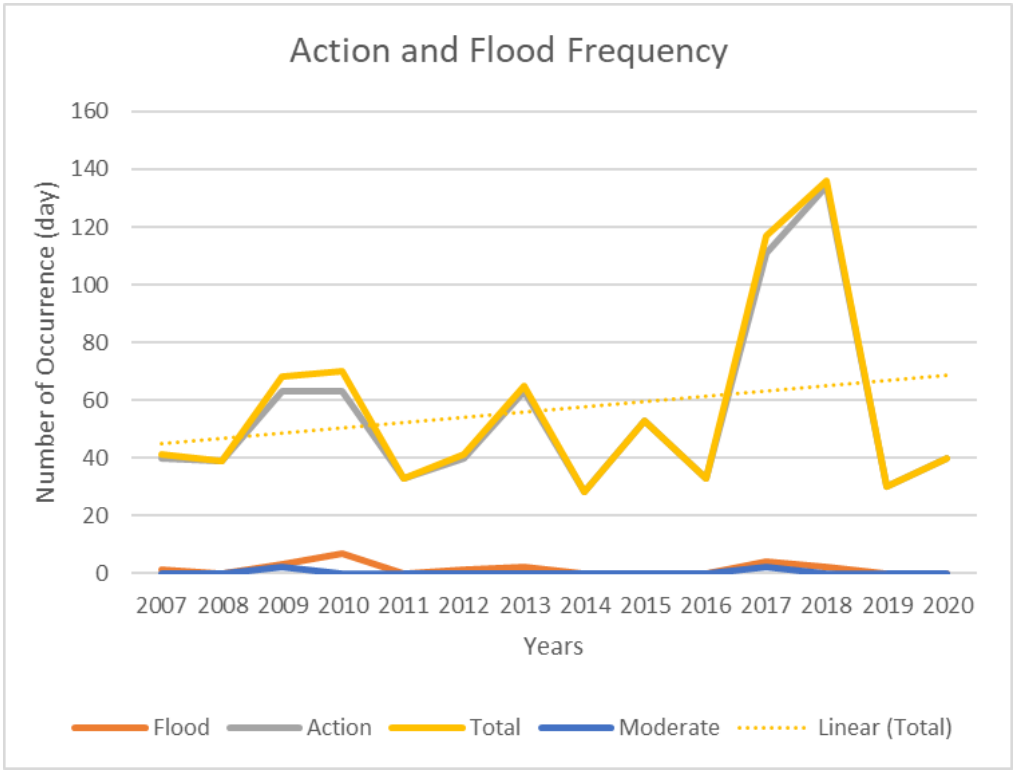
Action and Flood Frequency
Number of Occurrence (day)
160
140
120
100
80
60
40
20
0
2007 2008 2009 2010 2011 2012 2013 2014 2015 2016 2017 2018 2019 2020
Years
Flood
Action
Total
Moderate
Linear (Total)

Figure 15: (a) the flood frequency graph focuses on the gage heights which reach to flood and moderate level (b) the flood frequency graph focuses on the total gage heights which are above 5 (feet) in Potomac River.

(a)

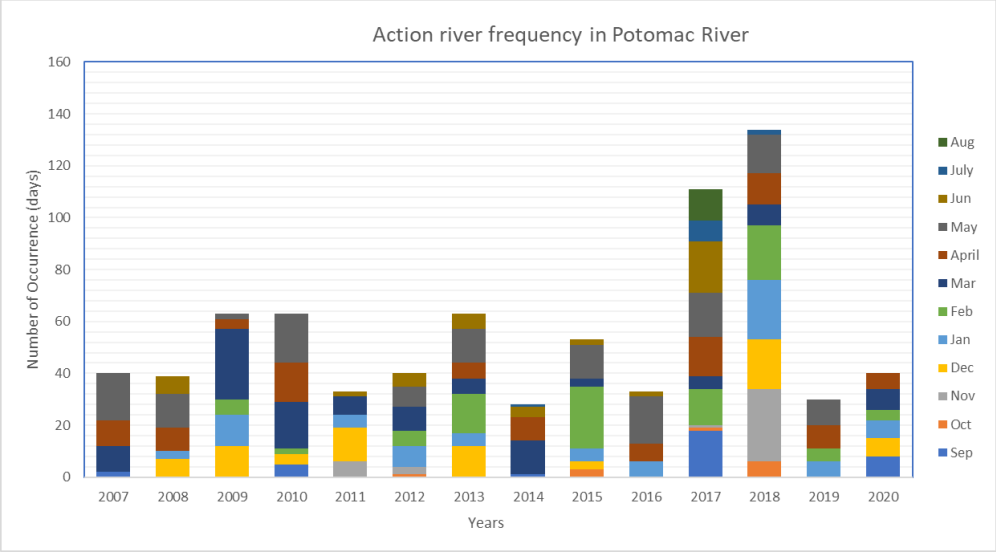

(b)

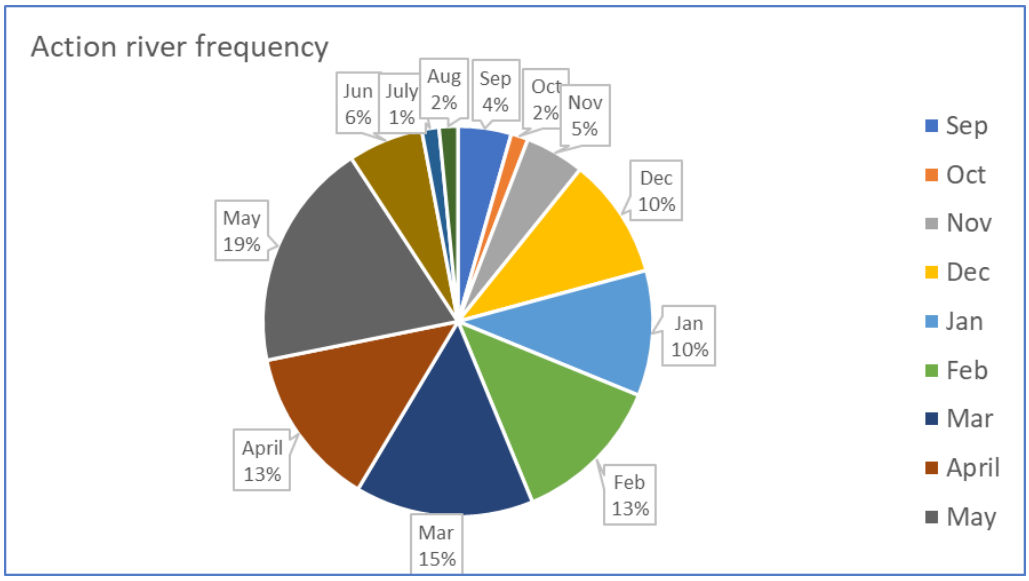

Figure 16: (a) The number of occurrences in each month for the gage heights from 2007 to 2021. (b) the percentage of the action flood occurrence in each month.

4.5 Air temperature and flood frequency

The study compares two figures to understand better the direct relationship between air temperature and flood frequency. Figure 17 (a) shows an apparent increase in air temperature from 2007 to 2019. The expectation would be that increasing air temperatures would lead to more rainfall and earlier snow melting, which could increase the likelihood of flooding. However, Figure 17 (b) shows a slightly negative relationship between air temperature and the occurrence of action water days, where increasing occurrences show a slight decrease in air temperature over the years.

(a)

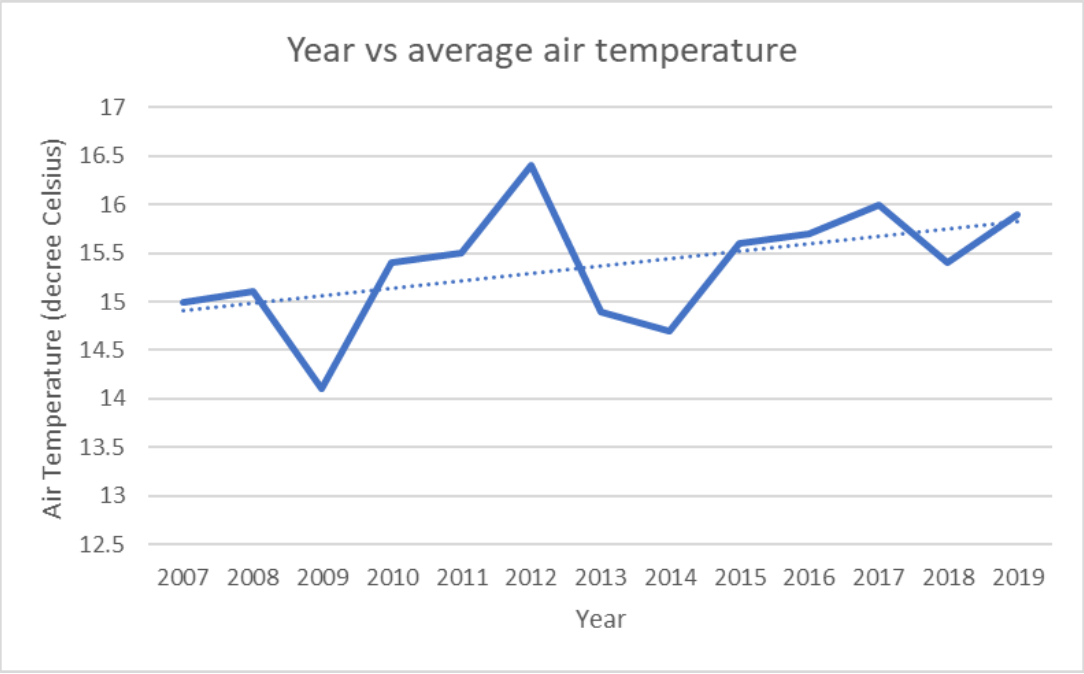

(b)

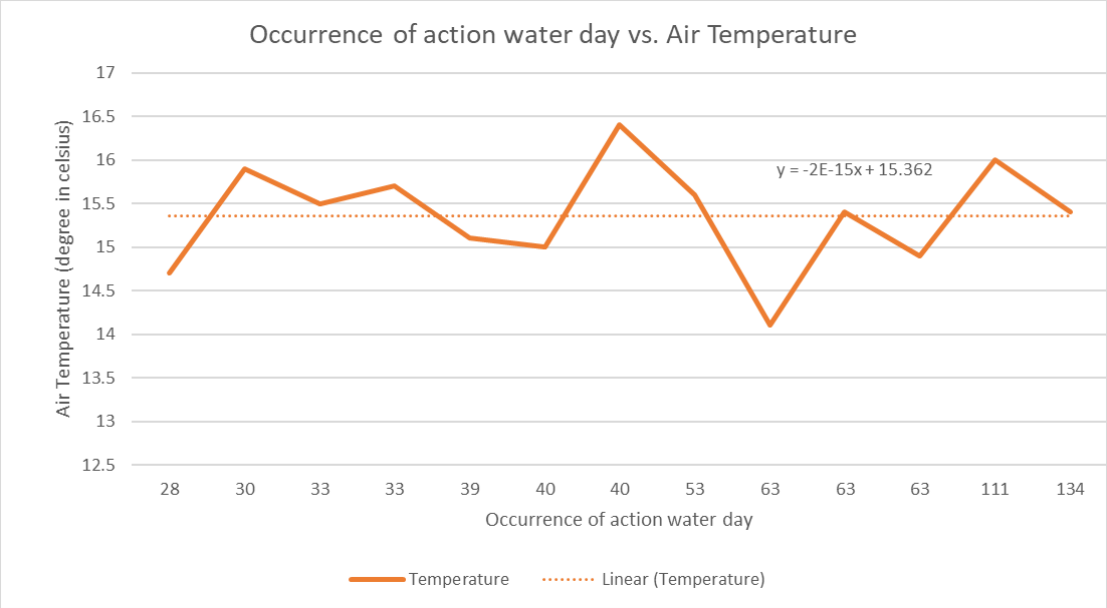

Figure 17 : (a) air temperature at Potomac River from 2007 to 2019. (b) Occurrence of flood and action water events verse of air temperature from less occurrence to frequently.

4.6 Monitoring the specific flood events and its vegetation

River Flooding

According to the National Weather Service, on 12 March 2020, light rain fell later in the morning, followed by heavier rain the next day. The most intense rain and sporadic thunderstorms occurred on 14 March, and showers continued until 15 March 2010 (National Weather). In order to detect the Normalized Difference Vegetation Index (NDVI) in this case, the MODIS satellite was initially selected. However, as shown in the left-side image of Figure 18 (a), the resulting NDVI was not as clear as the previous use of Sentinel-2. This expected difference in clarity is attributed to the significant difference in resolutions between the two

satellites. Resolution refers to the level of detail captured by a satellite sensor. A higher resolution means the sensor can capture finer details, whereas a lower resolution captures more generalized information but fewer details. In this case, the MODIS satellite has a resolution of approximately 250 meters, meaning it captures data in more significant and less detailed chunks compared to the Sentinel-2 satellite, which has a higher resolution of 15 meters. Because of this significant difference in resolution, the MODIS satellite is less capable of capturing finer and more detailed features on the ground, resulting in a less precise or more generalized NDVI image than the higher-resolution Sentinel-2 satellite. Therefore, a year-round NDVI plot was generated using Google Engine, as shown in Figure 18 (b). A significant dip in NDVI occurred immediately following January, likely due to the cold winter causing the leaves to fall. The NDVI value then increased again after the spring season. Focusing on the mid-March to April period, the NDVI increased sharply. While it may be partially accurate to assert that the NDVI increased after the flood event, the flood area was limited to Georgetown Park and Washington Harbor rather than the entire Washington area.

(a)

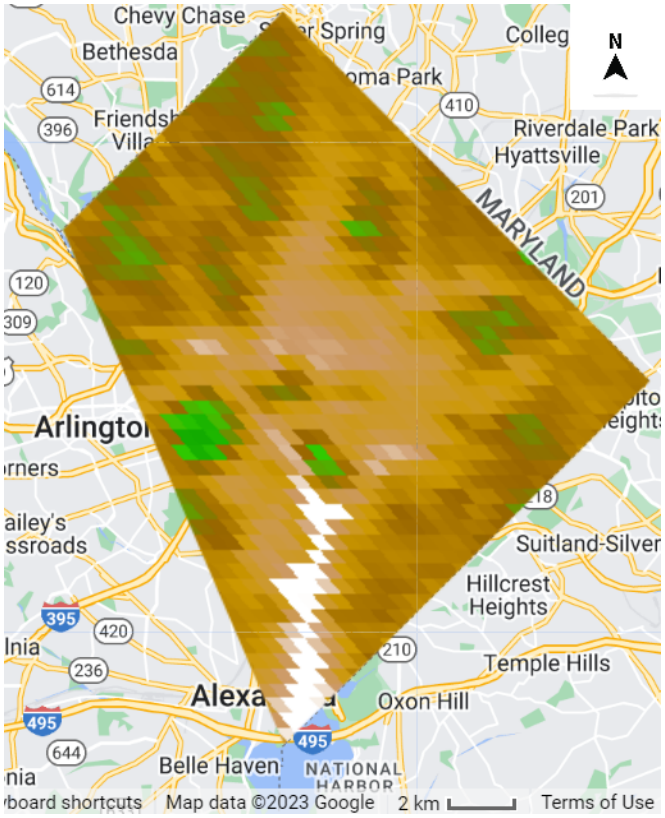
Chevy Chase
Bethesda
Spring
Colleg
oma Park
614
396
410
Riverdale Park
Hyattsville
201
MARYLAND
120
309
Arlingto
rners
ailey's
ssroads
18
Suitland-Silver
Hillcrest
Heights
395
420
lnia
236
210
Temple Hills
Alexa
Oxon Hill
495
644
495
Belle Haven
NATIONAL
HARBOR
N
board shortcuts
Map data ©2023 Google
2 km
Terms of Use

(b)

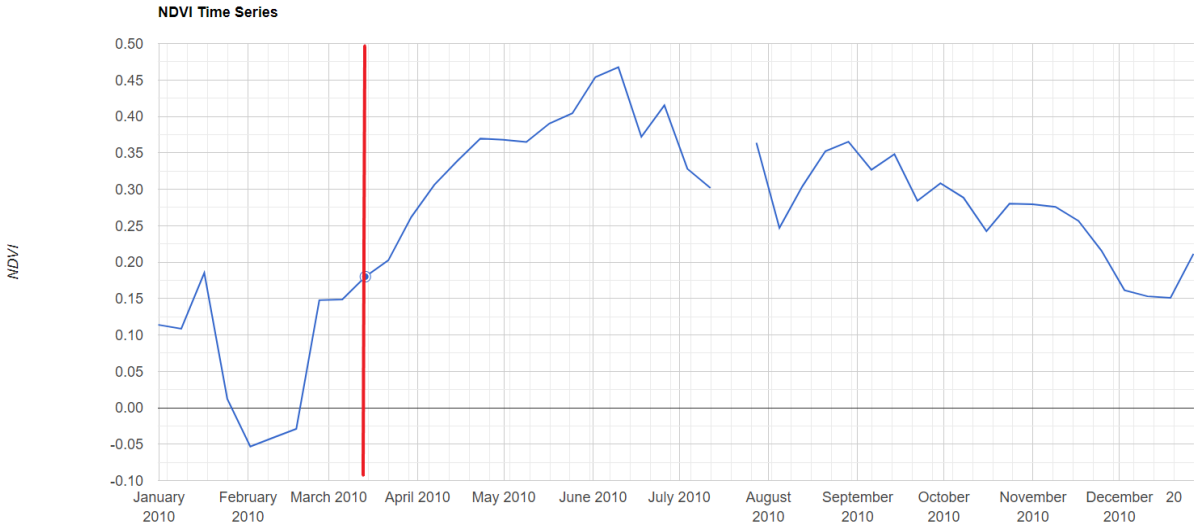
NDVI Time Series
NDVI
0.50
0.45
0.40
0.35
0.30
0.25
0.20
0.15
0.10
0.05
0.00
-0.05
-0.10
January 2010
February 2010
March 2010
April 2010
May 2010
June 2010
July 2010
August 2010
September 2010
October 2010
November 2010
December 2010
20

Figure 18: (a) the NDVI image in the Washington DC area, which was generated by MODIS. (b) the NDVI time Series for 2010 the whole year around.

Interior Flood Example on 2019 July 8

On July 8th, 2019, severe storms generated flooding in metro D.C. along the Potomac River. Nevertheless, it is challenging to accurately detect flooded areas on the day of the flood due to limitations imposed by the orbit of the satellites and their imaging capabilities. Remote sensing satellites use predefined orbits around the Earth, and their coverage of a specific spot is scheduled based on these orbital paths. This implies that the satellite might not pass over a particular area at the exact time of a flood event, making it challenging to catch real-time images during the peak of flooding. A post-flood image seems similar to a pre-flood image, which might be because the floodwaters have already receded (Figure 19). Figure 20 presents the NDVI (Normalized Difference Vegetation Index) before and after July 8th, with green representing vegetation areas and yellow representing urban areas. The NDVI was lower before the flood and higher after the flood, particularly around the Potomac River and downtown Washington, as shown in Figure 21. However, when looking closer at the left-side image of Figure 20, the Potomac River appears as a yellow area instead of the expected white color. To verify this discrepancy, USGS Earth Explorer was used, which revealed numerous clouds on the date chosen by Sentinel-2 prior to the flood event.

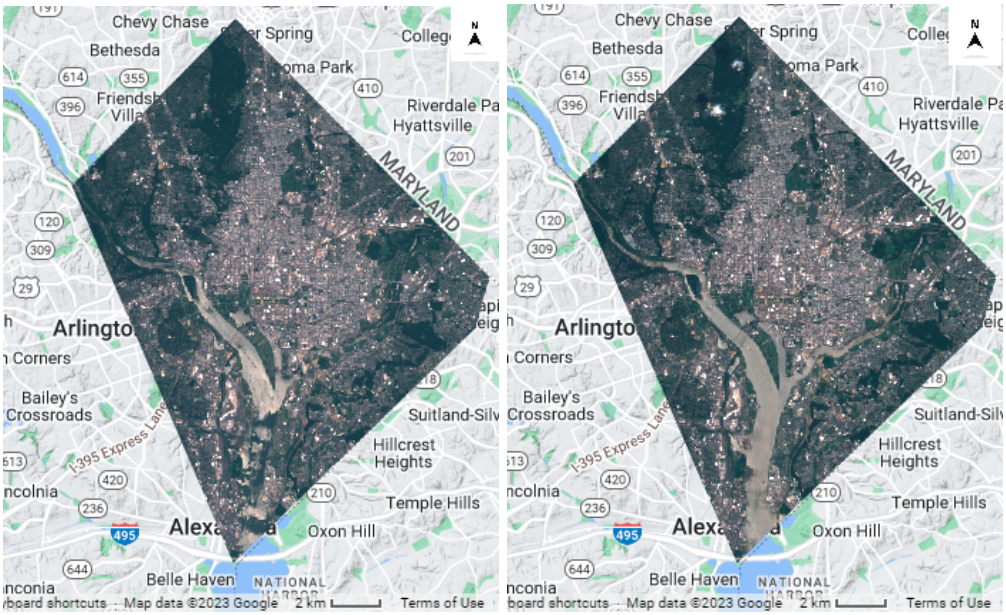

Figure 19: The radar image shows the land cover before (left), and after (right) the flood event occurred on July 8, 2019, by Sentinel-2.

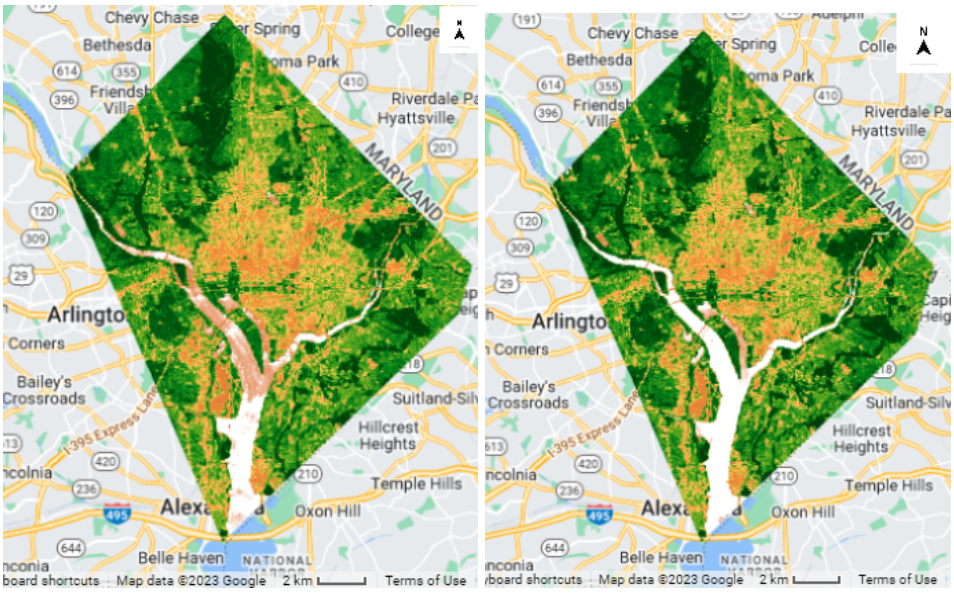

Figure 20: The image shows the NDVI before (left), and after (right) the flood event occurred on July 8, 2019, by Sentinel-2.

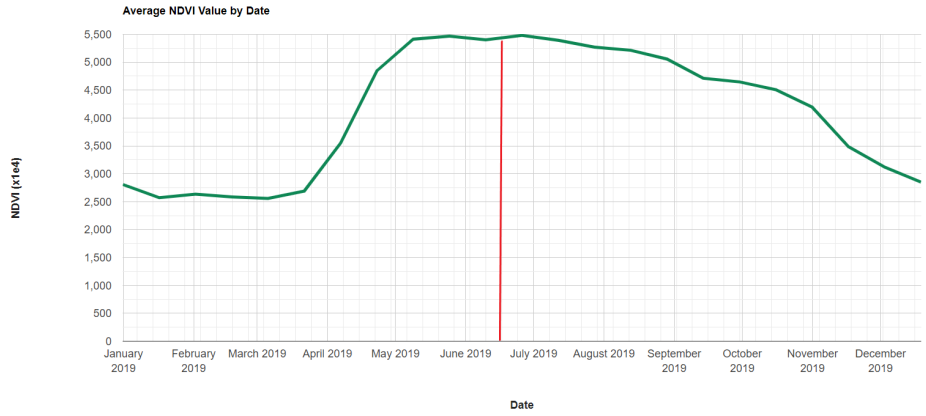

Figure 21: the NDVI image in the Washington DC area, which was generated by MODIS for the entire year of 2019, the red bar is showing the date of July 8.

Coastal flooding Example 2021 on Oct 26 at old town Alexandria

On October 26th, 2021, a storm impacted the area, directing to a widespread flood that impacted the coastal areas of Maryland, Virginia, Delaware, and New Jersey. The strong winds of the storm drove water into the Chesapeake Bay and Delaware Bay, causing significant flooding in these regions. A remote sensing radar captured compelling evidence, shown in Figure 23, revealing a notable difference in river conditions before and after the flood. The image displayed a significant increase in water volume at the bottom of the Potomac River following the heavy rainfall, indicating a concerning upward flow toward the urban vicinity.

The high salinity of the inundating water during coastal flood events theoretically leads to a decline in vegetation. This was supported by the NDVI analysis (Figure 22), which showed a

decrease in vegetation after the flood event (Figure 24). However, the drop in NDVI might also indicate plant senescence. In this natural process, plants age, and green foliage decreases, especially during the fall when not influenced by flood events. Understanding these ecological dynamics becomes critical in comprehending the potential long-term impact of the flood on the region's natural landscape.

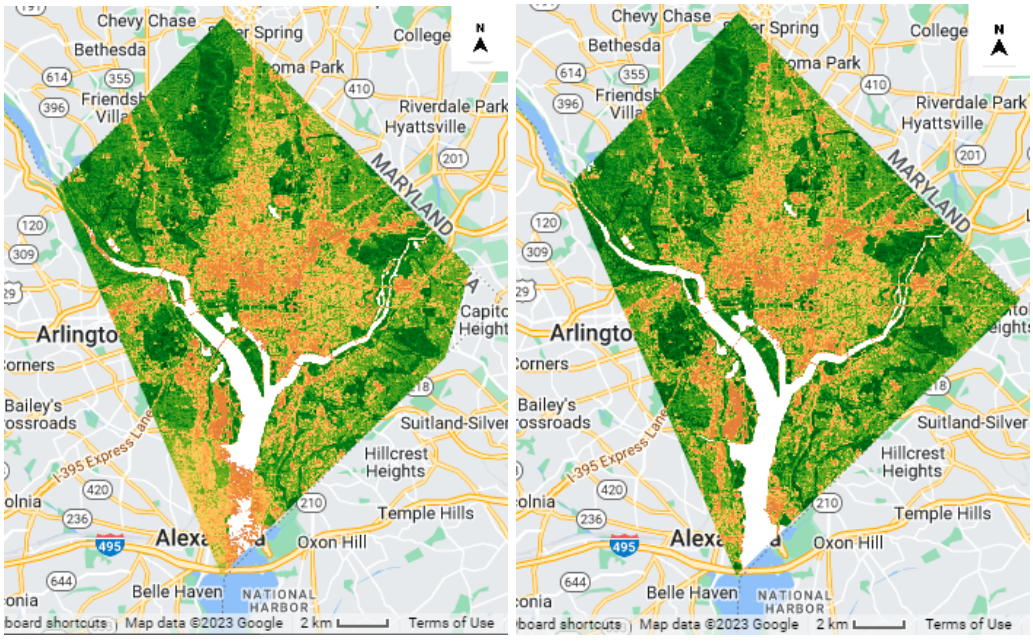

Figure 22: The image shows the NDVI before (left), and after (right) the flood event occurred on October 26, 2021, by Sentinel-2.

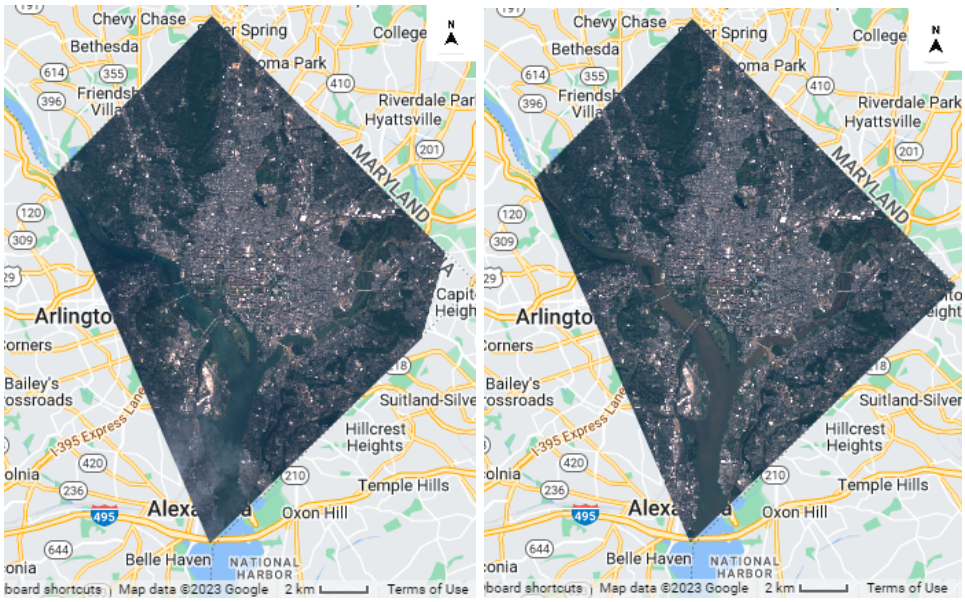

Figure 23: The radar image shows the land cover before (left), and after (right) the flood event occurred on 2021 Oct 26 by Sentinel-2 SAR.

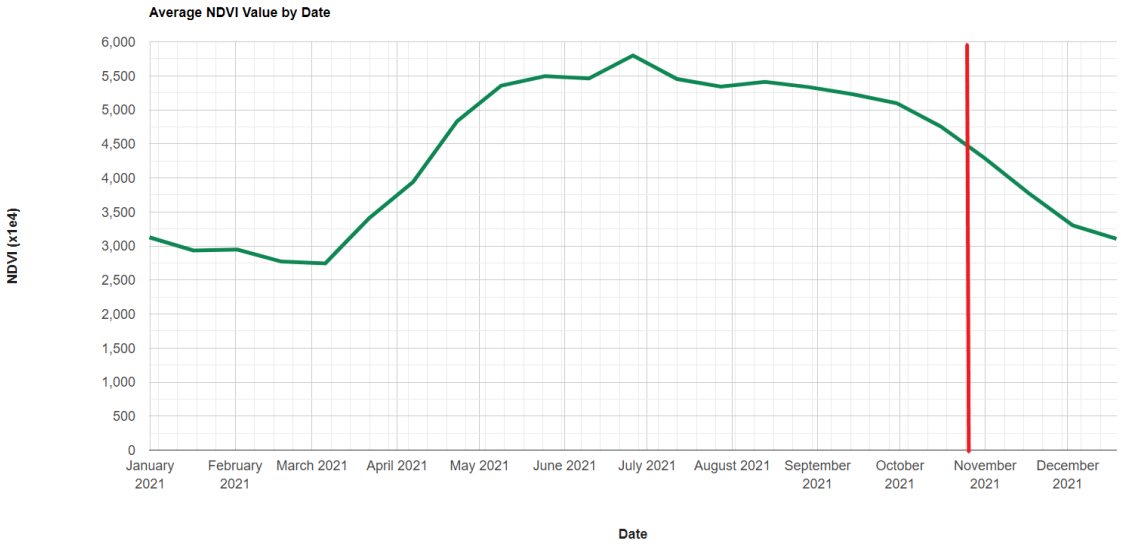

Figure 24: The upper left chart is the rainfall event right before the flooding event, and the upper right chart is the streamflow right before the flooding day. The bottom chart is the flood detection/intensity.

Land Classification with vulnerable area

To compare the state of the area before and after the October 24th, 2021 flooding event in the District of Columbia, land classification images were utilized (Figure 25). The land cover change was classified into different categories, with blue-colored areas representing permanent open-water areas, purple-colored areas indicating flooded vegetation during the event, and yellow and green-colored areas representing urban and vegetation areas. By classifying the land cover change, it became clear that the purple area is particularly vulnerable to flood events. This classification provides an efficient and rapid method of flood monitoring that could be beneficial for local administrations. However, it is important to note that obtaining remote sensing images during flooding can be challenging due to cloud cover. In such cases, other methodologies such as Synthetic Aperture Radar (SAR) could be employed, which is not affected by cloud cover and enables flood monitoring.

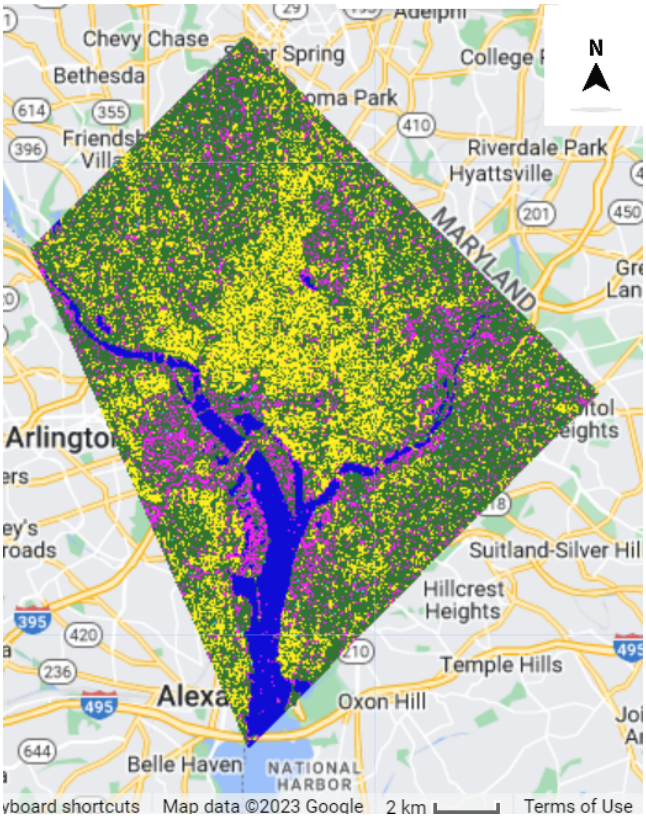

Figure 25: Land cover based on five classes (open water permanent (blue), open waterflood (light blue), flooded vegetation (purple), urban (yellow), and vegetation (green).) in Washington DC after 2021 OCT 26.

5. **Discussion**

The hypothesis is addressed that an increase in air temperature, sea level, and rainfall would result in more frequent floods, affecting vulnerable areas and vegetation. However, the data revealed a different scenario regarding higher temperatures and flood occurrences in the Potomac River. The relationship between air temperature and flooding is intricate and relies on regional climate patterns. Changes in land use or the construction of new infrastructure may also impact flood frequency.

The Potomac and Anacostia Rivers, located near Washington, DC, are susceptible to recurring floods. These floods can result in significant damage and loss of life. Hydrological measurements play a crucial role in determining flood insurance rates, facilitating emergency planning, and guiding infrastructure investments aimed at diminishing future flood risks. The rise in sea levels is predicted to intensify the occurrence of flooding events due to augmented ocean water levels. Consequently, low-lying coastal regions, particularly island areas, will face heightened vulnerability to extensive flooding resulting from sea-level rise. Active mitigation measures must be undertaken to safeguard the coastlines. The unplanned increases in urbanization and inadequate infrastructure make cities more vulnerable to urban floods. Remote sensing can help monitor the flooding area and determine how serious the flood would affect the area. This could help make more suitable strategies for urban disaster reduction, reduce the number of deaths related to disasters, and mitigate disaster damage to infrastructure.

The probabilities of various return period floods were examined for the Potomac and Anacostia Rivers. In the case of the Potomac River, the chances of experiencing a 100-year return period flood in any given year were calculated to be 1%. In contrast, for a 200-year return period flood,

the likelihood was found to be 0.5%. Correspondingly, for the Anacostia River, the annual probability of a 100-year return period flood was also defined to be 1%, and for a 200-year return period flood, the probability stood at 0.5%. Notably, the occurrence of a hundred-year flood stays constant at 1% in any given year, unaffected by past events. These probabilities provide vital senses for flood management and planning, helping assess risks and design appropriate flood control and water resource management strategies for the region.

The impact of hydraulic infrastructure in DC may have influenced flood frequency, with updated installations like improved drainage systems potentially mitigating flood risks. Coastal metropolises such as DC encounter distinctive challenges owing to their proximity to the ocean and vulnerability to sea-level rise. These challenges encompass a high population density, infrastructures in low-lying regions susceptible to flooding, unplanned urban development, coastal erosion, and substantial economic repercussions from floods. Coastal cities in the Northeast share similar flood frequency challenges and need comprehensive planning, resilient infrastructure investments, and collaboration to address these issues. Advanced technologies like remote sensing and real-time flood monitoring can aid in disaster preparedness and response, reducing the impact of floods on communities and infrastructure.

6. **Conclusion**

This research discusses the impact of climate change on flood frequency and intensity in Washington, DC, and its vegetation. The study carefully identifies areas at the highest risk and offers valuable insights into the relationship between sea-level rise and flood frequency. Additionally, it explores the diverse impacts of flooding on vegetation, ranging from positive to negative, while highlighting the key factors that influence these effects. The flood return curve (Figure 7) is a helpful tool for determining the probabilities of floods of different magnitudes. Based on historical records, this study can help predict the probability of future floods or water level events. The study reveals that high temperatures, directly and indirectly, impact water levels in the rivers, subsequently influencing flood intensity. Both the Potomac River and the Anacostia River have encountered temperature increases, further contributing to the complexity of their flood dynamics.

The flood frequency analysis is based on daily discharge and only includes 13 years of data on flood frequency and river activity. The study period may need longer, explaining the observed slight decrease in flood frequency. Many other factors can also influence flood frequency, such as storm activity, sedimentation, and water evaporation rates. Future studies should focus on the synergistic effects of both river systems on the DC area. Furthermore, the overall amount of water in the river has increased over the years. The data indicates that more action water days are associated with lower temperatures. This suggests that factors beyond just temperature are likely at play in determining flood frequency and also provides valuable insights into flood probabilities in the Potomac and Anacostia River areas. However, more research is needed to understand the complex factors influencing flooding in these regions fully.

Works Cited

Al'ala, M & Syamsidik 2019, 'Coastal Flooding Impacts Induced Sea Level Rise on Banda Aceh Coastal Morphology', *IOP Conference Series: Earth and Environmental Science*, vol. 273, no. 1, p. 012007.

Church, J. A., and White, N. J. (2011). Sea-Level Rise from the Late 19th to the Early 21st Century. *Surveys in Geophysics, 32(4-5), 585–602.* http://doi.org/10.1007/s10712-011-9119-.

Dahri, N., & Abida, H. (2020). Causes and impacts of flash floods: *case of Gabes City, Southern Tunisia. Arabian Journal of Geosciences, 13(4), 1-15.*

Dettinger, M 2011, 'Climate Change, Atmospheric Rivers, and Floods in California - A Multimodel Analysis of Storm Frequency and Magnitude Changes1', *JAWRA Journal of the American Water Resources Association, vol. 47, no. 3, pp. 514-523.*

Fuller, W. E.: Flood flows, T Am Soc Civ Eng, 77, 564– 617, doi:10.1061/taceat.0002552, 1914. 530 Gaál, L., Szolgay, J., Kohnová, S., Hlavčová, K., Parajka, J., Viglione, A., Merz, R., and Blöschl, G.: Dependence betweenflood peaks and volumes: *a case study on climate and hydrological controls, Hydrolog Sc J, 60, 968-984, doi:10.1080/02626667.2014.951361, 2015.*

Google Earth Engine. (2021). Google Earth Engine. Retrieved from https://earthengine.google.com/

Guan M, Wright NG, Sleigh PA, Carrivick JL. 2015. *Assessment of hydro-morphodynamic modelling and geomorphological impacts of a sediment-charged jökulhlaup, at Sólheimajökull, Iceland. Journal of Hydrology 530: 336–349.*

Haasnoot, M., Kwadijk, J., Van Alphen, J., Le Bars, D., Van Den Hurk, B., Diermanse, F., et al., 2020. Adaptation to uncertain sea-level rise; *how uncertainty in Antarctic mass-loss impacts the coastal adaptation strategy of The Netherlands. Environ. Res. Lett. 15 (3)* https://doi.org/10.1088/1748-9326/ab666c.

Hague, B. S., McGregor, S., Murphy, B. F., Reef, R., & Jones, D. A. (2020). Sea level rise driving increasingly predictable coastal inundation in Sydney, Australia. *Earth's Future*, *8*(9), e2020EF001607.

Held, I. M., & Soden, B. J. (2006). Robust responses of the hydrological cycle to global warming. *Journal of Climate, 19(21), 5686-5699. doi:10.1175/JCLI3990.1*

Hunt, J. C. R. (2005). Inland and coastal flooding: developments in prediction and prevention. *Philosophical Transactions of the Royal Society A: Mathematical, Physical and Engineering Sciences, 363(1831), 1475-1491.*

Intergovernmental Panel on Climate Change (IPCC). (2014). Climate Change 2014: Synthesis Report. *Contribution of Working Groups I, II, and III to the Fifth Assessment Report of the Intergovernmental Panel on Climate Change.*

Intergovernmental Panel on Climate Change (IPCC). (2018). Global Warming of 1.5°C. *An IPCC Special Report on the impacts of global warming of 1.5°C above pre-industrial levels and*

related global greenhouse gas emission pathways, in the context of strengthening the global response to the threat of climate change.

Karl, T. R., Meehl, G. A., Miller, C. D., Hassol, S. J., Waple, A. M., & Murray, W. L. (2008). Weather and Cliamte Extremes in a Changing Climate; Regions of Focus: North America, Hawaii, Caribbean, and U.S. Pacific Islands. *A Report by the U.S. Climate Change Science Program and the Subcommittee on Global Change Research. Washington, D.C., USA: Department of Commerce, NOAA's National Climatic Data Center.*

Lee, J. G., A. Selvakumar, K. Alvi, J. Riverson, J. X. Zhen, L. Shoemaker, and F. Lai. 2012. "A watershed-scale design optimization model for stormwater best management practices." *Environ. Modell. Softw. 37: 6-18.* doi.org/10.1016/j.envsoft.2012.04.011

Lionello, P., Nicholls, R. J., Umgiesser, G., and Zanchettin, D.: Venice flooding and sea level: past evolution, present issues, and future projections (introduction to the special issue), *Nat. Hazards Earth Syst. Sci., 21, 2633–2641*, https://doi.org/10.5194/nhess-21-2633-2021, 2021.

Little, C. M., Horton, R. M., Kopp, R. E., Oppenheimer, M., Vecchi, G. A., & Villarini, G. (2015). Joint projections of US East Coast sea level and storm surge. *Nature Climate Change, 5(12), 1114–1120.* https://doi.org/10.1038/nclimate2801

Liu, R. R., Gu, N. N., Li, G. D., and Wu, C. D. (2019a). Water quality assessment of Liuhe River based on single-factor standard index method. *J. Jianghan Univ. Nat. Sci. Ed. 2, 139–145. doi:10.16389/j.cnki.cn42-1737/n.2019.02.006*

López, L., Stahle, D., Villalba, R., Torbenson, M., Feng, S., & Cook, E. (2017). Tree ring reconstructed rainfall over the southern Amazon Basin. *Geophysical Research Letters,* 44, 7410–7418. https://doi.org/10.1002/2017GL073363

Mensah, H., and Ahadzie, D. K. (2020). Causes, impacts and copingstrategies of floods in Ghana: a systematic review. *SN Appl. Sci. 2, 792.doi: 10.1007/s42452-020-2548-z*

Merz, B., Blöschl, G., Vorogushyn, S., Dottori, F., Aerts, J. C. J. H., Bates, P., et al. (2021). Causes, impacts and patterns of disastrous river floods. *Nat. Rev. Earth Environ. 2, 592–609. doi: 10.1038/s43017-021-00195-3*

Metcalfe, J. (2016, March 30). The growth of impervious surfaces in Washington D.C. as seen by satellite. Bloomberg. Retrieved from https://www.bloomberg.com/news/articles/2016-03-30/the-growth-of-impervious-surfaces-in-washington-d-c-as-seen-by-satellite.

Mikhailova, M. V. (2021). Floods in the Venetian lagoon and their causes. *Water Resources, 48(5), 654–665. https://doi.org /10.1134/s0097807821050134.*

Naeem, M., Arif, M. S., Nawaz, A., Khalid, M. A., Jia, Y., Ding, Y., Chen, L., & Zhang, J. (2021). Waterlogging Induced Changes in Soil Properties, Root Growth and Morphology, and Nutrient Uptake in Brassica napus L. *Plants, 10(9), 1803.* https://doi.org/10.3390/plants10091803

National Climate Assessment. (2018). Impacts, Risks, and Adaptation in the United States: Fourth National Climate Assessment, Volume II. U.S. *Global Change Research Program.*

National Oceanic and Atmospheric Administration [NOAA]. (2021). Climate.gov: Science & Information for a Climate-Smart Nation. Retrieved from https://www.climate.gov/

National Oceanic and Atmospheric Administration [NOAA]. (2023). June 2023 Global Climate Report. Retrieved from https://www.ncei.noaa.gov/access/monitoring/monthly-report/global/202306-data

Ohba, M., Sugimoto, S. Differences in climate change impacts between weather patterns: possible effects on spatial heterogeneous changes in future extreme rainfall. *Clim Dyn 52, 4177–4191 (2019)*. https://doi.org/10.1007/s00382-018-4374-1

Pin-Chun Huang, An effective alternative for predicting coastal floodplain inundation by considering rainfall, storm surge, and downstream topographic characteristics. *Journal of Hydrology, Volume 607, 2022, 127544, ISSN 0022-1694,* https://doi.org/10.1016/j.jhydrol.2022.127544.

Ramsay, D., & Bell, R. (2008). Coastal hazards and climate change. *A Guidance Manual for Local Government in New Zealand, 2.*

Ray, T., Stepinski, E., Sebastian, A., & Bedient, P. B. (2011). Dynamic modeling of storm surge and inland flooding in a Texas coastal floodplain. *Journal of Hydraulic Engineering, 137(10), 1103-1110.*

Ruckert, K. L., Oddo, P. C., & Keller, K. (2017). Impacts of representing sea-level rise uncertainty on future flood risks: An example from San Francisco Bay. *PLoS ONE, 12(3), 1–17.* https://doi-org.eztncc.vccs.edu/10.1371/journal.pone.0174666

Singh, A. P., & Patil, A. S. (2021). Urban Floods-A Brief on Causes & Mitigation Management Strategies. *International Research Journal of Engineering and Technology. e-ISSN:2395-0056/p-ISSN:2395-0072.*

Singh, B. R., & Singh, O. (2012). Study of impacts of global warming on climate change: rise in sea level and disaster frequency. *Global warming—impacts and future perspective*.

Slater, L., and G. Villarini. 2016 update and expansion to data originally published in: Mallakpour, I., G. Villarini. 2015. The changing nature of flooding across the central United States. *Nature Climate Change 5:250–254.*

Sterr, H. (2008). Assessment of Vulnerability and Adaptation to Sea-Level Rise for the Coastal Zone of Germany. *Journal of Coastal Research, 24(2), 380–393.*

Sundaram, Sreechanth & Devaraj, Suresh & Yarrakula, Kiran. (2022). Mapping and Assessing Spatial Extent of Floods from Multitemporal Synthetic Aperture Radar Images: A Case Study over Chennai City, India. *10.21203/rs.3.rs-1565050/v1.*

Sweet, W., Park, J., Marra, J., Zervas, C., & Gill, S. (2014). Sea level rise and nuisance flood frequency changes around the United States.

Tabari, H. Climate change impact on flood and extreme precipitation increases with water availability. *Sci Rep 10, 13768 (2020).* https://doi.org/10.1038/s41598-020-70816-2

Tebaldi C, Ranasinghe R, Vousdoukas M, Rasmussen D J, Vega-Westhoff B, Kirezci E, Kopp R E, Sriver R and Mentaschi L 2021 Extreme sea levels at different global warming levels Nat. *Clim. Change 11 746–51.*

Vitousek, S., Barnard, P. L., Fletcher, C. H., Frazer, N., Erikson, L., & Storlazzi, C. D. (2017). Doubling of coastal flooding frequency within decades due to sea-level rise. *Scientific reports*, *7*(1), 1-9.

Walsh, K., Pittock, A. Potential Changes in Tropical Storms, Hurricanes, and Extreme Rainfall Events as a Result of Climate Change. *Climatic Change 39, 199–213 (1998).* https://doi.org/10.1023/A:1005387120972

Wu, B., Liu, Y., Wang, Z., Xu, X., Ma, L., Tang, J., & Zhang, H. (2022). Effects of flood frequency and intensity on sediment deposition and organic carbon storage in a riparian wetland of the Sanjiang Plain, China. *Catena, 209, 105537.* https://doi.org/10.1016/j.catena.2021.105537.

Xiaoxin Wang, Dabang Jiang, Xianmei Lang, Future extreme climate changes linked to global warming intensity, Science Bulletin, Volume 62, Issue 24, 2017, Pages 1673-1680, ISSN 2095-9273. https://doi.org/10.1016/j.scib.2017.11.004.

Yang Ju, Sarah Lindbergh, Yiyi He, John D. Radke, Climate-related uncertainties in urban exposure to sea level rise and storm surge flooding: a multi-temporal and multi-scenario analysis, Cities, Volume 92, 2019, Pages 230-246, ISSN 0264-2751.https://doi.org/10.1016/j.cities.2019.04.002.

Appendix

The frequency factors K table for log-Pearson Type III Distributions (Haan, 1977, Table 7.7)

	Recurrence Interval In Years							
	1.0101	2	5	10	25	50	100	200
SKEW COEFFICIENT Cs	Percent Chance (>=) = 1-F							
	99	50	20	10	4	2	1	0.5
3	-0.667	-0.396	0.420	1.180	2.278	3.152	4.051	4.970
2.9	-0.690	-0.390	0.440	1.195	2.277	3.134	4.013	4.904
2.8	-0.714	-0.384	0.460	1.210	2.275	3.114	3.973	4.847
2.7	-0.740	-0.376	0.479	1.224	2.272	3.093	3.932	4.783
2.6	-0.769	-0.368	0.499	1.238	2.267	3.071	3.889	4.718
2.5	-0.799	-0.360	0.518	1.250	2.262	3.048	3.845	4.652
2.4	-0.832	-0.351	0.537	1.262	2.256	3.023	3.800	4.584
2.3	-0.867	-0.341	0.555	1.274	2.248	2.997	3.753	4.515
2.2	-0.905	-0.330	0.574	1.284	2.240	2.970	3.705	4.444
2.1	-0.946	-0.319	0.592	1.294	2.230	2.942	3.656	4.372
2	-0.990	-0.307	0.609	1.302	2.219	2.912	3.605	4.298
1.9	-1.037	-0.294	0.627	1.310	2.207	2.881	3.553	4.223
1.8	-1.087	-0.282	0.643	1.318	2.193	2.848	3.499	4.147
1.7	-1.140	-0.268	0.660	1.324	2.179	2.815	3.444	4.069
1.6	-1.197	-0.254	0.675	1.329	2.163	2.780	3.388	3.990
1.5	-1.256	-0.240	0.690	1.333	2.146	2.743	3.330	3.910
1.4	-1.318	-0.225	0.705	1.337	2.128	2.706	3.271	3.828
1.3	-1.383	-0.210	0.719	1.339	2.108	2.666	3.211	3.745
1.2	-1.449	-0.195	0.732	1.340	2.087	2.626	3.149	3.661
1.1	-1.518	-0.180	0.745	1.341	2.066	2.585	3.087	3.575
1	-1.588	-0.164	0.758	1.340	2.043	2.542	3.022	3.489
0.9	-1.660	-0.148	0.769	1.339	2.018	2.498	2.957	3.401
0.8	-1.733	-0.132	0.780	1.336	1.993	2.453	2.891	3.312
0.7	-1.806	-0.116	0.790	1.333	1.967	2.407	2.824	3.223
0.6	-1.880	-0.099	0.800	1.328	1.939	2.359	2.755	3.132
0.5	-1.955	-0.083	0.808	1.323	1.910	2.311	2.686	3.041
0.4	-2.029	-0.066	0.816	1.317	1.880	2.261	2.615	2.949
0.3	-2.104	-0.050	0.824	1.309	1.849	2.211	2.544	2.856
0.2	-2.178	-0.033	0.830	1.301	1.818	2.159	2.472	2.763
0.1	-2.252	-0.017	0.836	1.292	1.785	2.107	2.400	2.67
0	-2.326	0.000	0.842	1.282	1.751	2.054	2.326	2.576

	Recurrence Interval In Years							
	1.0101	2	5	10	25	50	100	200
SKEW COEFFICIENT Cs	Percent Chance (>=) = 1-F							
	99	50	20	10	4	2	1	0.5
0	-2.326	0.000	0.842	1.282	1.751	2.054	2.326	2.576
-0.1	-2.4	0.017	0.846	1.27	1.716	2.000	2.252	2.482
-0.2	-2.472	0.033	0.850	1.258	1.680	1.945	2.178	2.388
-0.3	-2.544	0.050	0.853	1.245	1.643	1.890	2.104	2.294
-0.4	-2.615	0.066	0.855	1.231	1.606	1.834	2.029	2.201
-0.5	-2.686	0.083	0.856	1.216	1.567	1.777	1.955	2.108
-0.6	-2.755	0.099	0.857	1.200	1.528	1.720	1.880	2.016
-0.7	-2.824	0.116	0.857	1.183	1.488	1.663	1.806	1.926
-0.8	-2.891	0.132	0.856	1.166	1.448	1.606	1.733	1.837
-0.9	-2.957	0.148	0.854	1.147	1.407	1.549	1.660	1.749
-1	-3.022	0.164	0.852	1.128	1.366	1.492	1.588	1.664
-1.1	-3.087	0.180	0.848	1.107	1.324	1.435	1.518	1.581
-1.2	-3.149	0.195	0.844	1.086	1.282	1.379	1.449	1.501
-1.3	-3.211	0.210	0.838	1.064	1.240	1.324	1.383	1.424
-1.4	-3.271	0.225	0.832	1.041	1.198	1.270	1.318	1.351
-1.5	-3.33	0.240	0.825	1.018	1.157	1.217	1.256	1.282
-1.6	-3.880	0.254	0.817	0.994	1.116	1.166	1.197	1.216
-1.7	-3.444	0.268	0.808	0.970	1.075	1.116	1.140	1.155
-1.8	-3.499	0.282	0.799	0.945	1.035	1.069	1.087	1.097
-1.9	-3.553	0.294	0.788	0.920	0.996	1.023	1.037	1.044
-2	-3.605	0.307	0.777	0.895	0.959	0.980	0.990	0.995
-2.1	-3.656	0.319	0.765	0.869	0.923	0.939	0.946	0.949
-2.2	-3.705	0.330	0.752	0.844	0.888	0.900	0.905	0.907
-2.3	-3.753	0.341	0.739	0.819	0.855	0.864	0.867	0.869
-2.4	-3.800	0.351	0.725	0.795	0.823	0.830	0.832	0.833
-2.5	-3.845	0.360	0.711	0.711	0.793	0.798	0.799	0.800
-2.6	-3.899	0.368	0.696	0.747	0.764	0.768	0.769	0.769
-2.7	-3.932	0.376	0.681	0.724	0.738	0.740	0.740	0.741
-2.8	-3.973	0.384	0.666	0.702	0.712	0.714	0.714	0.714
-2.9	-4.013	0.390	0.651	0.681	0.683	0.689	0.690	0.690
-3	-4.051	0.396	0.636	0.660	0.666	0.666	0.667	0.667